

Abstract

Williams, James Alfred. Characteristics of Replacement Lithography and Desorption on Various Metal Substrates. (Under the direction of Professor Christopher B. Gorman)

The development of molecular electronic systems relies on the investigation of metal/molecule interactions. A popular methodology to forming metal/molecule interfaces uses the formation of self-assembled monolayers (SAMs), SAMs are capable of forming consistent, well order single to multiple layers of molecules oriented with respect to surface characteristics. While a plethora of techniques exist for exploring this phenomenon the utilization of replacement lithography presents a systematic approach to investigating the formation and stability of SAMs on various substrates. However, in authenticating investigations using lithographic techniques, the employment of electrochemistry forms conclusions on desorption and adsorption characteristics of the SAMs. While contemplating the contribution posed by metal/molecule interactions the facilitation of comparative methodologies in rationalizing processes of altering the characteristics of the monolayers, provides a speculative vantage of future endeavors into the development of molecular electronics.

**CHARACTERISTICS OF REPLACEMENT LITHOGRAPHY AND
DESORPTION
ON VARIOUS METAL SUBSTRATES**

by
JAMES ALFRED WILLIAMS

A thesis submitted to the Graduate Faculty of
North Carolina State University
in partial fulfillment of the
requirements for the Degree of
Master of Science

CHEMISTRY

Raleigh

2004

APPROVED BY:

Christopher B. Gorman
Chair of Advisory Committee

Dedication

To my family, friends, and teachers

BIOGRAPHY

JAMES ALFRED WILLAMS was born in Fayetteville, North Carolina on May 6, 1980. Born into the military family of Michael and Mary Williams, he lived in many different states and the Philippines along with his brother and sister, Michael and Rebecca. Nearing the end of his father's military career, the family returned to North Carolina. James proceeded with his education at Cape Fear High School graduating salutatorian in 1998. While in high school, he also attended Fayetteville Technical Community College to gain college credit in Statistics, Civil War History, and Sociology. After graduating, James attended Campbell University majoring in Mathematics and Chemistry in the spring of 2001. The following fall, he began attending the Graduate Program at North Carolina State University.

Acknowledgments

I would like to thank Dr. Christopher Gorman for his guidance in the conceptualization and preparation of this project. In addition, I would to thank Ryan Furrier, Drew Wassel, Stephan Kraemer, Holly Robuck, and Grace Credo for sharing the potential of scanning tunneling microscopy and introducing me to the world on molecular electronics. Also, I express my appreciation to Matt Lewis for his aid in discuss and preparation of replacement lithography methodologies. Finally I would like to express my gratitude towards the rest of the Gorman's group for their aid in my preparation of reductive desorption experiments especially Chris Cameron, Tyson Chase, and Angela Allen.

TABLE OF CONTENTS

FIGURE LIST	VII
LIST OF TABLES	XI
CHAPTER I PRINCIPLES OF MOLECULAR ELECTRONICS.....	1
1. ELECTRONICS	2
1.1. PRINCIPLES GOVERNING THE PN JUNCTION	3
1.1.1. <i>Bipolar Transistors</i>	4
1.1.2. <i>Field Effect Transistor</i>	5
1.2. INTRODUCTION TO MOLECULAR ELECTRONICS	8
1.2.1. <i>Study of Metal/Organic Surface Interactions</i>	10
1.3. CONCLUDING THOUGHTS	13
CHAPTER II CHARACTERISTICS OF SURFACE PROPERTIES.....	15
2. SURFACE CHEMISTRY	16
2.1. ADSORPTION METHODOLOGIES	16
2.2. FACETED SURFACE	19
2.4. PRINCIPLES OF STM	22
2.4.1. <i>Molecular approaches to characterizing SAMs</i>	24
2.5. CONCLUSIONS	27
CHAPTER III REPLACEMENT LITHOGRAPHY.....	29
3. REPLACEMENT LITHOGRAPHY.....	30
3.1. CAUSES OF VARIATIONS	33
3.2. VARIOUS SUBSTRATES	35
3.2.1. <i>Surface Characteristics</i>	36
3.2.2. <i>Effect of Surface Oxides</i>	38
3.3.3. <i>Transconductance</i>	40
3.4. CONCLUSIONS.....	41
3.5. EXPERIMENTAL DESIGN.....	41
3.5.1. <i>Fabrication of Substrates and Preparation of Monolayer</i>	41
3.5.2. <i>Procedure for Replacement Lithography</i>	42
3.6. PROGRAMS	43
3.6.2. <i>Variation of Voltage</i>	43
3.6.3. <i>Variation of Scanning Bias for Transconductance</i>	44
CHAPTER IV STUDY OF REDUCTIVE DESORPTION.....	46
4. ELECTROCHEMICAL ADSORPTION & DESORPTION.....	47
4.1. DESORPTION OF ALKANE THIOLS ON GOLD	49
4.2. ELECTROCHEMISTRY OF ELECTROACTIVE MOLECULES PLATINUM AND GOLD SUBSTRATES... 50	
4.3. ELECTROCHEMICAL DESORPTION ON PLATINUM AND GOLD SUBSTRATES.....	52
4.4. CONCLUSIONS	53
4.5. EXPERIMENTAL PROCEDURE	54
4.6. REFERENCES	56
APPENDIX I SCHEMES OF STM CELL DESIGN	57
AI.1 STANDARD CELL DESIGN	57
AI.2 RAISED BOLT CELL DESIGN.....	57

AI.3 IMBEDDED CELL DESIGN.....	58
AI.4 SEALED CELL DESIGN.....	58
AI.5 NEVER LEAK CELL DESIGN.....	59
APPENDIX II SCHEMES OF ELECTROCHEMICAL ELECTRODE	60
AII.1. INDIUM CONTACT ELECTRODE.....	60
AII.2. SILVER CONTACT ELECTRODE.....	60
AII.3. TOP CONTACT ELECTRODE.....	60
AII.4. PLASTI™-DIP ELECTRODE.....	60
AII.5. DMF ANNEALED ELECTRODE.....	61

Figure List

Chapter I Principles of Molecular Electronics

Figure 1.1. - a) Schematic of a pn junction and its voltage characteristics b) Illustrates the application of a more positive voltage to the p-type region of the pn junction c) Shows the application of a more negative bias3

Figure 1.2. - A schematic of a pnp-bipolar transistor.....4

Figure 1.3. - Truth table illustrating basic concepts of electronic. (F) represents forward biasing with respect to the base junction (R) represents reverse biasing with respect to the base junction (E,C,B) illustrate emitter, collector, and base.....5

Figure 1.4. - A schematic of a MOSFET device.....6

Figure 1.5. - a) A diagram of $\text{Co}(\text{typ}-(\text{CH}_3)_5\text{-SH})_2$ b) I-V curves at varied gate bias c) The schematic diagram of a device with the measurement setup is shown.¹9

Figure 1.6. - 1) 9,10-di(20-(para-acetylmercapto-phenyl)ethinyl)-anthracene
2) 2,5-di(20-(para-acetylmercapto-phenyl)ethinyl)-4-nitro-acetylaniline⁶11

Figure 1.7. - Contact resistance, R_0 , as a function of metal work functions for alkanethiol junctions. The effective work functions of mixed metal pairs are taken to be the average of the two metal work functions. The solid line is a guide for the eye.⁷12

Chapter II Characteristics of Surface Properties

Figure 2.1. - The stacking structure of the LB film. Triangles denote donor molecules and circles represent acceptor molecules.¹.....17

Figure 2.2. - Tilt angle with respect to vertical position for thiols on gold.....18

Figure 2.3. - a) A representation of a face centered cubic (fcc) unit cell common to gold, palladium, and platinum. b) A fcc unit cell cut through the [111] axis to illustrate a crystallographic representation of a (111) plane. c) An illustration of (111) lattice structure that uses a $\sqrt{2}/2$ atomic spacing to form a terrace. Sites 1, 2, and 3 represents binding sites which can be characterized by coordinate systems respective to adjoining molecules.....20

Figure 2.4. - (a) LEED pattern obtained for an incident energy of 40 eV for dodecane thiol on Au(111). The surface temperature was 150K. Preparation was via the thermal treatment (430 K) of films that were deposited from ethanolic solution. (b) Calculated LEED pattern, corresponding to a $p(13 \times \sqrt{3})$ structure. The three different symbols (Δ , \bullet , \square) denote three domains rotated by 120° with respect to each other. (c) Same as (a), but for an incident energy of 42.5 eV and the dodecane thiol was vapor deposited at 150 K, heated to 330 K and cooled again to 150 K. (d) Same as (b), but corresponding to a $c(27 \times \sqrt{3})$ structure.⁷21

Figure 2.5. - a) Scheme of STM. b) Movement pattern of tip across surface.....22

Figure 2.6. - Constant-current images for a Au(111) substrate, which has been immersed for 24 h into a 100 μ M solution of BP3 in ethanol at 333 K. Three different rotational domains corresponding to the Au(111) substrate symmetry are indicated by arrows. An enlarged image demonstrating molecular resolution is shown in panel b. Tunneling parameters: (a) U) 1 V, I) 600 pA; (b) U) 0.59 V, I) 110 pA.⁸25

Chapter III Replacement Lithography

Figure 3.1. - (A) Initial scanning setting designed to observe SAMs without perturbing the monolayer. (B) Desorption of the monolayer into solution as a result applied potential. (C) Replacement of the monolayer with substituted molecules into desorption sites. (D) Return to initial scanning parameters.....30

Figure 3.2 - Apparent height difference of electroactive thiols at varying imaging biases under dodecane. The letters “Fc” were written with Fc-C11SH, and the letters “Gal” were written with Gal-C6SH. RC: 3.0 V, 10 pA, 50 nm/s; RH, 59%. IC: 600x600 nm, 3 nm z scale, 10 pA, 1 Hz scan rate. Imaging bias: (A) 115 mV, (B) 700 mV, and (C) 1800 mV¹.....32

Figure 3.3 - Images of replacement lithography labeled with respect to perspective substrate metal and replacing molecule is (Fc-C₁₁SAc) into dodecanethiolate monolayer. Imaging conditions: Au and Pd 1.7 V scan bias, 10pA, and 3nm Z range; Pt 1.9V scan bias, 10pA, and 3 nm Z range. RL conditions: ~55% relative humidity and biases of 3.4V, 3.1V, 3.55V respectively written at 20nm/s within replace regions. A) Pit region within the monolayer surrounded by visible lines called domain boundaries.....35

Figure 3.4 - A graphic representation of the Percentage of Fc-C₁₁SAc Replacement versus Replacement Bias (the line is meant to guide the eye through mean percentage of each bias). Adjacent images represent data points for the graph with lines generated as a result of Voltage biases listed above each line with respective substrate indicated by adjacent labeled graph. Gold, platinum, and palladium substrate imaging conditions $V_{bias} = 1.7V$ scale=350nm², $V_{bias} = 1.9V$ scale=400nm², $V_{bias} = 1.7V$ scale=350nm² respectively. All setpoint and Z-scale were 10pA and 3nm.....37

Figure 3.5 - Graphs of Percentage of Fc-C₁₁SAc Replacement versus Replacement Bias of un-etched platinum and palladium. A) Pd C₁₂S monolayer imaged a 1.0V, setpoint 10pA, scan size 400 nm², and 3nm Z-scale.....**39**

Figure 3.6 - Above images reveal the effect of varying applied bias on the replaced molecule (Fc-C₁₁S) on various substrates labeled in bottom right of each images with scan bias listed to the right with respect to lined in regions.....**40**

Chapter IV Study of Reductive Desorption

Figure 4.1. - Cyclic voltammograms for reductive desorption of self-assembled monolayers composed of alkanethiolates recorded under the same conditions with those in Figure 1. The number of methylene units is indicated by each curve. Curves are for annealed SAMs except for curve 4.¹.....**49**

Figure 4.2. - Schematic depiction of electrode surface modified by with an osmium thiol monolayer .⁴.....**51**

Figure 4.3. - Cyclic Voltammograms of the reductive desorption of dodecane and decane thiol monolayers on gold and platinum substrates labeled respectively. Taken at a scan rate of 100mV s⁻¹ , after 3 hours of under potential deposition at -200mV.....**52**

Appendix I Schemes of STM Cell Design

Figure A1.1. - Schematic of basic STM Cell design using platinum ball with foil stem A) Teflon well with hallow center and recessed inner ring. B) Ferromagnetic stainless steel disc 6 holed for screw attachment to Teflon well. C) Rubber o-ring used to create leak resistant seal. D) Platinum ball with foil stem.....**56**

Figure A1.2. - Schematic of raised bolt STM Cell design using platinum ball with foil stem A) Teflon well with hallow center and recessed inner ring. B) Ferromagnetic stainless steel disc 6 holed for screw attachment to Teflon well. C) Rubber o-ring used to create leak resistant seal. D) Stainless steel nut used to secure platinum foil to setup E) Elongated metallic screw.....**56**

Figure A1.3. - Imbedded Screw design. A) Casing of an AFM cell with threaded bottom inner shaft. B) Threaded bottom for mounting screw. C) Epoxy Seal to secure screw and prevent leakage. D) Dodecane and FcC₁₁SH solution. E) Screw and nut imbedded in epoxy to anchor the substrate. F) Ferromagnetic disk attached with conductive ink.....**57**

Figure A1.4. - Sealed Cell Design. A) Machined metal casing made from ferromagnetic stainless steel. The bottom of which contains a hole for the screw. B) Resin solder used to seal the bottom of the cell and secure the screw. C) Standard Screw bolt design with platinum foil. D) Dodecane and FcC₁₁SH solution.....**57**

Figure AI.5. - Never Leak Design. A) Machined metal casing made from ferromagnetic stainless steel. The bottom of which contains a threaded hole for the screw with a beveled bottom. B) Screw sealed with conductive ink. C) Platinum or Palladium Substrate using a wire based form of attachment. D) Dodecane and FcC_{11}SH solution...**58**

Appendix II Schemes of Electrochemical Electrode

Figure AII.1. - Indium Contact Electrode. A) Copper wire used to make electrical contact. B) Substrate of choice: Pt, Pd, or Au.....**59**

Figure AII.2. - Silver Conductive Ink Electrode. A) Copper wire used to make electrical contact. B) Hot glue used to stabilize wire. C) Tygon tubing used to secure electrode to cell setup. D) Glass casing used to deliver conductive ink and shield wiring. E) Conductive ink creating interface between substrate and copper wiring. F) Substrate....**59**

Figure AII.3. - Top Contact Electrode. A) Glass cell created by melting the end and sanding end to reveal micron size hole. B) Vacuum Grease sealant. C) Annealed so that faceted surface aligns with glass frit (D). E) Reference electrode. F) Counter electrode. G) Electrolyte solution.....**59**

Figure AII.4. - Plasti™-Dip Electrode A) Working Electrode. B) Reference electrode. C) Counter electrode. D) Plasti™-Dip coating isolates electrolyte solution and limits exposure to faceted region.....**59**

Figure AII.5. - A) Flame annealed ball for 15 min to maximize faceted regions. B) Counter electrode. C) Quasi-reference electrode (Pt wire).....**60**

List of Tables

Chapter III Replacement Lithography

Table 3.1 - List of work functions with respect to substrate and orientation. ¹¹	38
--	-----------

Chapter I

Principles of Molecular Electronics

1. Electronics

The birth of modern electronics has created various avenues for the development of our society. Modern electronics can be seen in the way that we communicate with each other, in the way that we perceive the world, and even the way we cook our food. Yet, even with modern electronics at their current state; there is a need to improve these systems by making them faster, smaller and more energy efficient which has become a driving force for our society. As these systems improve, certain physical limits are being uncovered based on limitations of classical physics. This has led to the necessity in creating an understanding of molecular electronics; however, attempting to grasp the concept of molecular electronics creates a need for a firm understanding of basic electronics. The key factors of basic electronics provide a means for describing objectives in the establishment of a new system of molecular electronics.

While attempting to cover the basics of electronics, several areas will be investigated. The first of these areas will include the basic concepts and properties of positive and negative substrate (pn) junctions. In order to further expand upon this topic, will require a glimpse into field effect transistors and interfaces between metals and semiconductors. Presenting an avenue into characterizing molecular electronic devices based on electronic modeling theories similar to that of Park's application of a molecular device to simulate a single electron transistor (SET) device will be used.

1.1. Principles Governing the pn Junction

The pn junction of modern electrical systems relies upon several basic components and principles. Components for pn junctions consist of p-type and n-type substrates, in which the ‘type’ of substrate depends upon the dopant implanted into the substrate. For instance in order to ascertain a p-type substrate of silicon, the implantation of boron or aluminum ions is relatively common. Conversely, n-type substrates commonly use the insertion of phosphorus or arsenic ions. The relationship between dopants and the type of substrate is determined by the ion affinity of the implanted molecules relative to the substrate. Hence, the addition of p-type dopants creates positive charges in the substrate commonly referred to as holes. Conversely, with n-type substrates the dopant adds electron rich regions to the substrate.

Pn junctions emerge as a result of p-type and n-type substrates being imbedded adjacent to each other. Once the pn junction forms, holes and electron rich regions diffuse from their respective substrates. Creating a potential difference (V_{dep}) between the two substrates, thus a separation of charge on opposite sides of a “layer devoid of charge

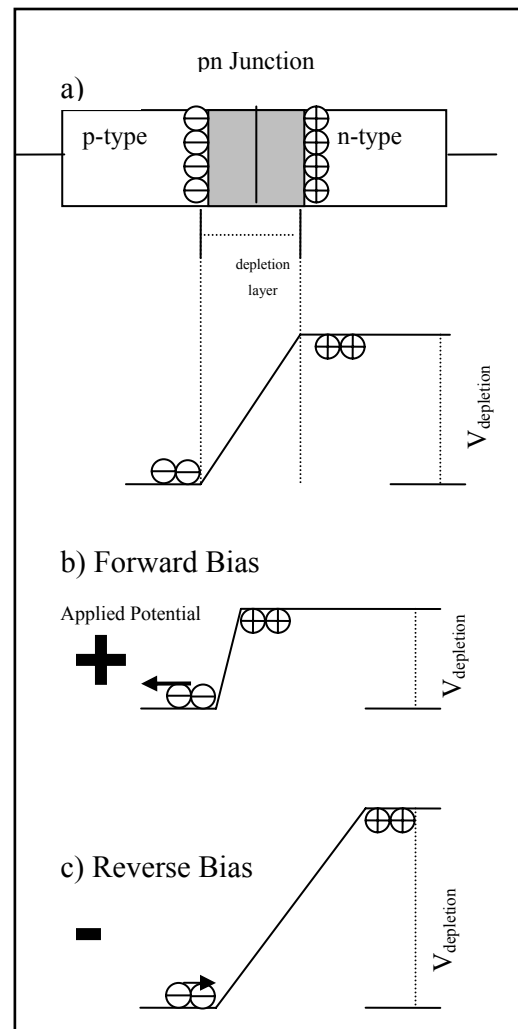


Figure 1.1 a) Schematic of a pn junction and its voltage characteristics b) Illustrates the application of a more positive voltage to the p-type region of the pn junction c) Shows the application of a more negative bias

carriers”¹ called the depletion layer are formed (Figure 1.1a). The depletion layer plays a pivotal role in controlling the flow of current through the pn junction. For instance, as seen in Figure 1.1b, when the more positive potential is applied to the p-type side of the junction; current flows readily between the junctions due to a narrowed depletion layer. Narrowing the depletion layer results from a compensation due to the removal of defused electrons from the p-type region.¹ A phenomenon known as forward biasing the junction. Reverse biasing the system requires that the depletion layer widens as extra electrons are added to the p-type region (Figure 1.1c). Thus, creating a leakage current which becomes restricted as the applied potential increases causing a limitation to the current that can flow through the junction.¹ It is this dual state ability that makes pn junctions so important to the development of modern electronics.

1.1.1. Bipolar Transistors

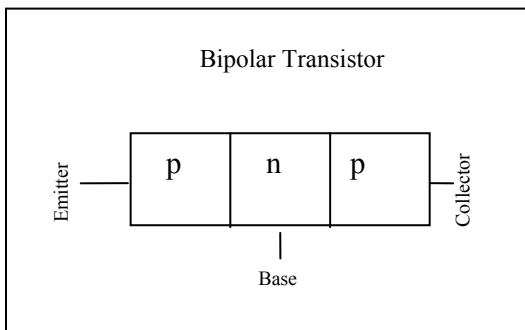


Figure 1.2 A schematic of a pnp-bipolar transistor

Transistors serve multiple functions in electronics through the control of electrical current. They are capable of amplifying current flow, turning the current on or off, and providing a means of electronic logic.

Transistors can amplify the flow of current, when considering the example where the emitter acts as the input current region and the collector as the output. By reverse biasing the Emitter/Base Junction and forward biasing the Base/Collector junction creates a leakage current from the emitter to collector (Figure 1.2). This system allows the collector to remove the incoming electrons from the saturated emitter/base depletion layer, thereby amplifying the current. Also, notable is

the base controls the amplification process by controlling the biasing of both the emitter and collector junctions. Controlling the bias leads to the ability of turning the current flow from the emitter to collector on or off. By reverse or forward biasing both of the junctions the base can turn off the current, which in turn allows the creation of electronic logic.

Electronic logic depends upon having more than one transistor, in order to create a series of logical outcomes as seen in (Figure 1.3). Of course, more connections are

required than shown in this simple schematic. However, as a representation of an ‘OR’ logical device, it illustrates that with one transistor closing the flow of current

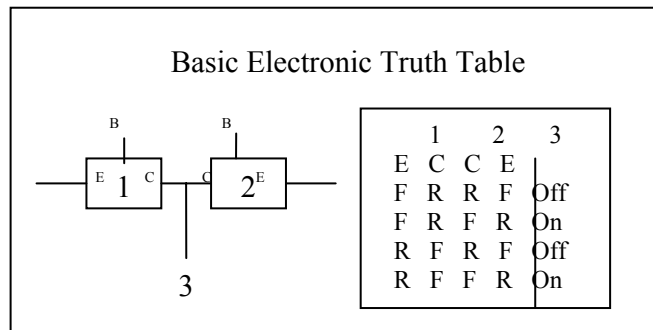


Figure 1.3 Truth table illustrating basic concepts of electronic. (F) represents forward biasing with respect to the base junction (R) represents reverse biasing with respect to the base junction (E,C,B) illustrate emitter, collector, and base

the device can still function if the other transistor is open to current flow. Hence, transistors produce a

source of many possible combinations using transistors in different arrangements to simulate logical functions. Thus, the application of transistors reveals a versatile avenue on which modeling molecular electronic devices can be achieved.

1.1.2. Field Effect Transistor

As a conclusion to basic concepts of electronic it is essential to explore the uses of metal/semiconductor devices in the form of field-effect transistors (FET). Oxner explains “the field-effect transistor is a class of electronic semiconductor device in which the conduction of a ‘channel’ between source and drain terminals is controlled by an

electric field impressed upon the channel via a gate terminal.”² In the illustration of a

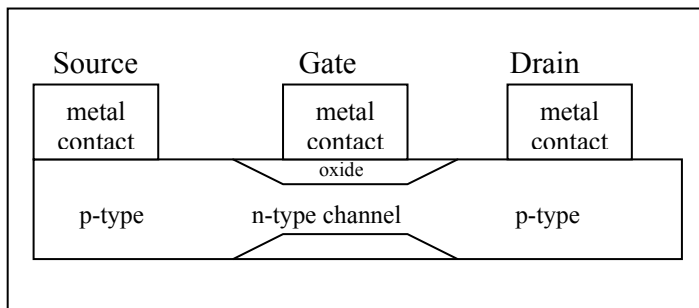


Figure 1.4 A schematic of a MOSFET device

metal oxide semiconductor FET

(Figure 1.4), the gate applies an

electric field in order to control

the flow of current. The oxide

that exists between the gate and

the n-type channel allows for

the forward and reverse biasing of the system without the adding the effect of leakage

current as seen in bipolar transistors. Without the effect of leakage current MOSFETs

are able to operate at greater energy efficiency and produce less heat due to energy

dissipation during switching. On the other hand, MOSFET devices are still able to

amplify the current flowing through the channel by increasing the gate bias to make the

n-type channel more accessible to the system.

MOSFETs have unique electronic properties which can be scaled down in

dimensions in order to create microscopic circuitry. With this ability has come the

development of modern electronic chips which contain millions of MOSFET transistors

within a few square centimeters capable of processing large amounts of data each

second. Using the electronic logic previously mentioned, these transistors are fabricated

in large arrays to create vast network-able functions called integrated circuits. Yet, there

are physical limitations to how far the transistors can be scaled down. For instance, as

the channel length decreases, so must the gate oxide thickness; but as the gate oxide

approaches the nanometer regime classical physics ceases to apply and quantum physics

takes over. A concept of quantum physics known as tunneling occurs when the distances

between two conductive layers approaches the nanometer regime and electrons are allowed to pass through the potential barrier. Tunneling current through the oxide layer prevents the proper functions of the FET. However, another limitation to scaling down transistors lay in photolithographic techniques.

Photolithography utilizes light to form patterns on the silicon substrate to create integrated circuits through the use of a mask and photo-activated fluids known as photoresists. Two types of photoresist, negative and positive, are used in industry to produce the dimensional patterns on microchips. Negative photoresist patterns regions that are unexposed to a given light source by removing the exposed regions. The light source depends on the dimensional parameters sought and the abilities to dissociate the photoresist. In contrast, positive photoresists are used to remove the exposed regions. The mask determines which regions are exposed to the light; however, since the mask is a set distance from the substrate and since light has wave-like properties, the mask must have smaller pattern dimensions than that of the substrate. This is one of the problems of photolithography; another exists in the light source itself. To maintain the high resolution required to create submicron integrated circuits, lower wavelength light sources are required. For instance, Intel used “248 nm and 193 nm lithography” to produce 250 to 180 nm scale dimensions, but are working toward 13.4 nm in order to pattern “below 50nm dimensions.”³ However “light at this wavelength does not travel through the atmosphere and is absorbed by glass.”³ This presents a problem since large scale vacuums are expensive to maintain and mirrors are used in order to target the light sources. These difficulties create a growing need for molecular electronics to facilitate the demand for faster, smaller, more energy efficient transistors.

1.2. Introduction to Molecular Electronics

While studying metal/organic interactions, a common approach to characterizing this system relies on dividing it into simpler, more manageable components. While this method does not allow one component to dictate the behavior of the entire system; it presents avenues for exploring various aspects of these interactions. This philosophy has led to many studies that focus on the molecule that attaches to the metal surface; presenting a vast assortment of arrangements to study with diverse approaches in forming metal/organic devices that can be classified as “molecular devices.” Molecular devices are structures that utilize a nanometer scale setup to control the flow of electrons between junctions such as: nanowires, nanotubes, molecular wires, and self-assembled monolayers. These components are then used to form molecular devices that provide an avenue to studying the effect of electric fields on a molecular scale.

A common approach to creating molecular devices exploits the creation of nanometer scale gaps that can be “filled” with molecules that may contain interesting electronic properties. The nanometer gap fabrication can consist of various methods. Park et al. utilized the creation of gold nanowires on top of “an aluminum gate with 1-2 nm native oxide”, “lithographically defined on a silicon oxide surface.”⁴ Nanowires are wires of essentially pure metals confined to submicron thickness, in Park’s case the wires were approximately 30 nm thick. In this instance, the thickness of the nanowire dictated the success of characterizing molecular junctions since thicker wiring might have allowed several molecules to assemble within the gap altering the single electron transistor model

by allowing multiple tunneling events to occur. The thickness of nanowires would have had two effects on the setup; multiple molecules would have altered the effect of the gate bias on the system creating alternate sources of current flow. The wire thickness also creates another possible effect, variation in binding distances from the gate allowing the molecules to create potential differences in current-voltage (I-V) curves. In the experiment, Park's group avoided these variations by using a diluted concentration of insert molecules. However with the use of diluted concentrations, molecules were "found in less than 10% of the electrodes," representing a low success rate but confirms "that it is unlikely to have multiple molecules across one gap."⁴

Park's et al. system used a cobalt complex with two tpy-(CH₂)₅-SH end groups (Figure 1.5a), allowing for a model similar to a single electron transistor (SET) device. SET devices function by creating a potential well that only one electron can occupy at a time, with a potential barrier imposed on the electron that inhibits it from leaving the well; until it is overcome through increasing the bias of the system. Thus, creating a staircase effect of the voltage bias as each electron moves through the system. This phenomenon called "coulomb blockade" is depicted in Park group's current-voltage measures of the cobalt complex

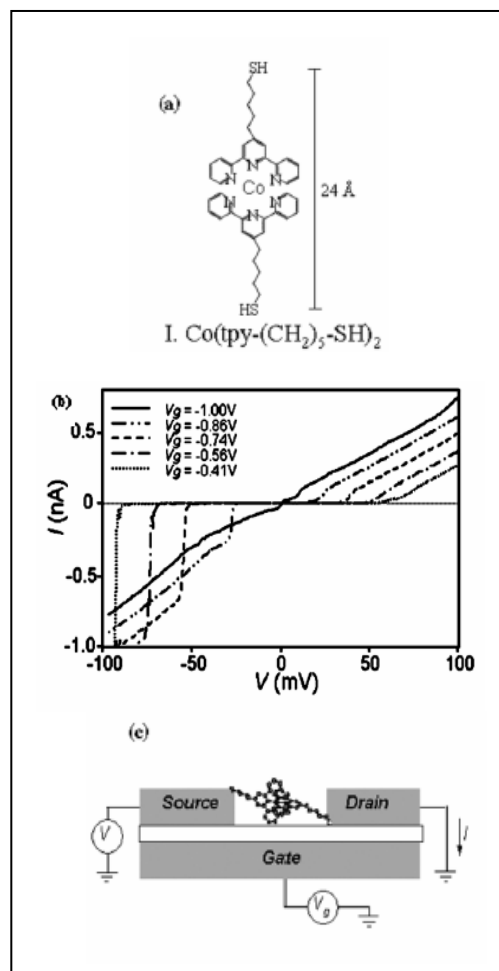


Figure 1.5 a) A diagram of $\text{Co}(\text{tpy}-(\text{CH}_2)_5\text{-SH})_2$ b) I-V curves at varied gate bias c) The schematic diagram of a device with the measurement setup is shown.⁴

illustrated in Figure 1.5b. Molecular devices, such as Park's et al. in Figure 1.5c illustrate a common theme in the analysis of these devices by explaining I-V characteristics through the use of basic electronic schemes. Thus, imposing a need for the understanding of basic electronic in order to model these devices, and create a novel approach to molecular electronics.

1.2.1. Study of Metal/Organic Surface Interactions

Sequentially to properly make use of molecular devices, details of the effects of metal/organic interactions on the device become necessary. Requiring a similar approach as used in Section 1.2, many aspects of surface interactions are analyzed using an assortment of techniques. Techniques to study this phenomenon range from using nano-gaps in the form of break junction devices, creating self-assembled molecular FET, to measuring properties of surface monolayers by atomic force microscopy (AFM) or scanning tunneling microscopy (STM). Break junction devices consists of submicron diameter wires placed on a pivoting point, in order to create a break in the wire that can be filled using the chemisorption of tailored molecules. 'Wiring' of molecules allows for a direct measure of relative electronic properties as a relation to the individual structural properties of the molecule. However, this provides uncertainties as to the exact attachment of the number of molecules. For instance, when a molecule is bound to a surface it exhibits a three orders of magnitude better conductance than an unbound molecule.⁵ This underlining theory applies to large potential ranges unlike the work of Weber's group; in which a gold break junction contained 9,10-di(20-(para-acetylmercapto-phenyl)ethinyl)-anthracene (Figure 1.6.1) or 2,5-di(20-(para-acetylmercapto-phenyl)ethinyl)-4-nitro-acetylaniline (Figure 1.6.2) were formed.⁶

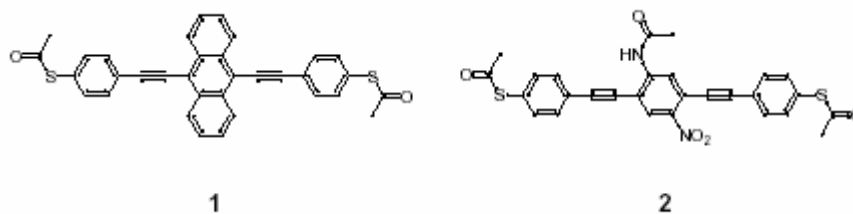


Figure 1.6 1) 9,10-di(20-(para-acetylmercapto-phenyl)ethynyl)-anthracene
 2) 2,5-di(20-(para-acetylmercapto-phenyl)ethynyl)-4-nitro-acetylaniline⁶

Weber et al. used this design to examine the effects of distance on tunneling current and uses the significant increases in current to explain the attachment of single and multiple molecules between the electrodes. Once the attachment of one or more molecules was confirmed, current-voltage (I-V) curves were obtained under vacuum to characterize the electronic properties of the molecules. The data reveals a correlation between the symmetric characteristics of the molecules and symmetric I-V curves enabling for a distinction between the setups. For instance, symmetric molecule 1 gave symmetric I-V data while molecule 2 did not.⁶ Concluding that the I-V data resulted from the molecular structure and not “experimental artifacts like water layers on the surface or anything else.”⁶ Also, the symmetry of I-V data presented a model in which molecules can be examined by being bound to one electrode and not the other, generating comparable results to that of a scanning tunnel microscope.⁶ Weber group’s setup created a scheme that allowed an interpretation of metal/organic interactions.

A key aspect of metal/organic interactions lies in the alterations of the electronic properties of molecules as a result of binding to the surface. Methods of measuring the conductance of molecules bound to a surface relies on the ability to make adequate contact to both ends of the molecule; for this reason AFM provides a direct measurement of molecular conductance. The importance of establishing the conductance of molecules

in relation to their bound state will play a pivotal roll in the creation of molecular electronic devices; since, the most common approaches to creating molecular devices relies upon creating metal/organic/metal structures on top of semi-conductive surfaces. Beebe et al. explored conductivity experiments using conductive atomic force microscopy (C-AFM) with metal coated AFM tips. These experiments were designed to measure the contact resistance of monolayers with different functionalized anchoring groups and different metal substrates. The functionalized anchoring groups varied between thiols and isonitriles of various Carbon chain lengths. Contact resistance of the monolayers was achieved by plotting the semi log resistance versus Carbon chain lengths and the point at which the plot intersects the resistance axis. When comparing the contact resistance Beebe's group found that there was a 10% decrease in the contact resistance

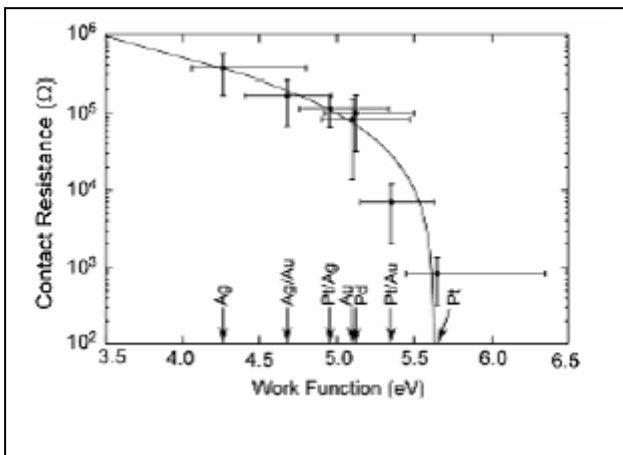


Figure 1.7 Contact resistance, R_0 , as a function of metal work functions for alkanethiol junctions. The effective work functions of mixed metal pairs are taken to be the average of the two metal work functions. The solid line is a guide for the eye.⁷

between isonitriles and thiols when each are bound to a gold substrate.⁷ Which demonstrated isonitriles greater effectiveness in binding to gold through Fermi contact compared to that of thiols and gold. Also a comparison was made through the variation of substrates from Pt, Pd, Ag, and Au. By changing the substrate and tip metals, a variation in the Fermi

levels occurs as result of alterations in work functions. Beebe et al. found that as the work function increased with change in substrate a decrease in contact resistance

resulted. The decrease of the contact resistance was perceived as a lowering of the barrier height with the increase in the Fermi level respective to the work function. In order to establish a better understanding of metal/organic interactions requires theoretical calculations to explore the effects of Fermi interactions and contact resistance.

1.3. Concluding Thoughts

While a basic understanding of electronic systems creates an avenue into the development of theories in molecular electronic systems. The establishment of MOSFETs role in modern electronic demonstrates a need for a molecular electronic system in which electron tunneling does not provide a hindrance to the system, rather is utilized for the creation of electronic logic. In order to develop methodologies in the fabrication of molecular devices, surface interactions between metal substrates and organic molecules must be characterized. Avenues to studying these interactions consist of establishing a firm understanding of surface science. Through the conceptualization of the development of surfaces, formation of organic films, and investigation of various interactions, surface science begins to explain practicalities of molecular devices. Hence to further examine surface interactions effect on molecular systems, the utilization of methods and the setup of samples to analyze these systems become imperative.

1.4. References

- (1) G. Pridham. Solid-State Circuits Pergamon Press (1973) 9.
- (2) E. Oxner. Designing with Field-Effect Transistors. McGraw-Hill Publishing Company, (1990) 1.
- (3) <http://www.intel.com/research/lithography.htm> 12/2/2003
- (4) J. Park, A. Pasupathy, J. Goldsmith, A. Soldatov, C. Chang, Y. Yaish, J. Sethna, H. Abruña, D. Ralph, P. McEuen. *Thin Solid Films* 438 –439 (2003) 457–461.
- (5) D. Vuillaume, S. Lenfant. *Microelectronic Engineering* 70 (2003) 539-550.
- (6) H.B. Weber, J. Reichert, F. Weigend, R. Ochs, D. Beckmann, M. Mayor, R. Ahlrichs, H.v. Löhneysen. *Chemical Physics* 281 (2002) 113–125.
- (7) J. Beebe, V. Engelkes, L. Miller, C. Frisbie. *J. Am. Chem. Soc.* 124 (2002) 11268–11269.

Chapter II

Characteristics of Surface Properties

2. Surface Chemistry

A principle component of nanotechnology rests in the study of surface chemistry to reveal the interactions between the surfaces and the adsorbed molecules. Attaching molecules to the surface are possible through several routes of adsorption. Chemisorption, physisorption, and Langmuir-Blodgett are methods of forming arrangements of molecules that can be analyzed through probing of the molecular/surface interface. In order to explore aspects of these interactions several avenues of surface chemistry must be explored. Before an analysis of a molecular device can begin surface substrates in which the molecular can adsorb must be fabricated. With the fabrication of a surface compatible for use in the investigation, the methodology of attachment comes into question. Enabling the study of these surfaces requires the use of various spectroscopic techniques or electronic devices. STM provides an avenue into exploring the electronic densities of the surface through the study of surfaces created through faceting metals. However, a deeper understanding of this process will allow a better method to characterizing the surface/molecule interface.

2.1. Adsorption Methodologies

The fabrication of molecular devices relies upon the ability to create a setup that remains stable under various environmental conditions. Environmental factors including heat, oxidation, static discharge, and surface stress make the formations of stable devices a challenging exploration. Several techniques provide a means for creating a variety of self-assembled nanostructures on surfaces. These self-assembled monolayers (SAMs) possess variations in physical, chemical, and electrical properties based on their interactions with the surface interface and each other. The state in which the monolayer

or array of molecules adsorb upon the surface directly dictates its characteristics. Whether the SAMs forms as a result of direct chemical binding to the surface know as chemisorption; or resulting from interacting with the structural properties know as physisorption a determination of the binding state prior to analysis becomes necessary in order to reveal information regarding characteristics that are applicable to molecular structural properties. Thus, SAMs present a vast range of study-able systems to characterize possible avenues of molecular setups.

One particular example of Langmuir-Blodgett (LB) SAMs utilizes a technique of immersing the substrate into a solution containing donor-acceptor tailed and non-polar chain terminated characteristics. These molecules align upon the surface in a manner that creates polarized and non-polarized ends as the

substrate is removed from solution with an applied pressure. The donor-acceptor tailed terminal group consists of an electron donor and electron acceptor moiety that is separated by an alkyl group (see Figure 2.1). These distinctive

end groups allow multiple layers to assemble upon the monolayer. However without binding to

a surface, Langmuir-Blodgett monolayers lack the uniformity that exists with an atomically flat region. The lack of uniformity produces defects throughout the monolayer. While defects like gaps or disorder regions exist in all monolayers, fabricating organic FET through the use of Langmuir-Blodgett (LB) requires a minimal amount of defects to prevent the deposition of metals through the SAM. Organic FET

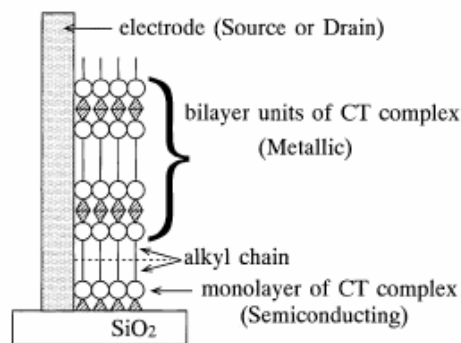


Figure 2.1. The stacking structure of the LB film. Triangles denote donor molecules and circles represent acceptor molecules.¹

such as those created by Sakuma et al.¹ presents a means to bypass the deposition of metals through the LB monolayer by prefabricating the substrate as seen in Figure 2.1. The use of prefabricated substrates elevates many inconsistencies providing a reproducible method of characterizing LB films. Due to instability of the formation of LB films, thickness of the multilayer, and limitations of possible systems of study, STM measurements would provide little insight into these systems.

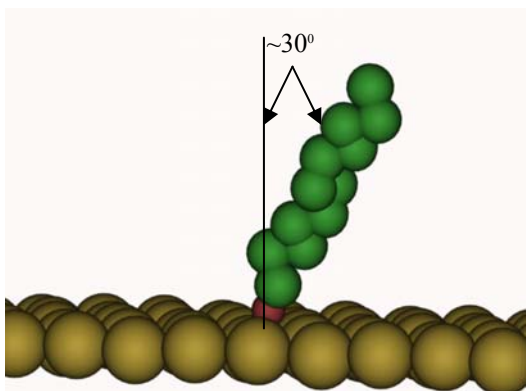


Figure 2.2 Tilt angle with respect to vertical position for thiols on gold.

The use of chemisorption in the formation of monolayers presents various opportunities to utilize molecular analysis in the characterization of monolayer formation as a result of highly ordered, close packed SAMs. For instance in several studies that characterize the binding of thiols to gold revealed that binding occurs at an angle to

the surface (see Figure 2.2).²⁻⁴ While the actual tilt angle of the molecules depends upon its molecular structure, a common tilt of at least 30 degrees occurs as a direct result of the van der Waals interactions amongst bound molecules. The direct binding of the monolayer to the surface provides an advantage of a higher conductance when compared to physisorbed monolayers.⁵ The higher conductance of the monolayer presents an example of the alteration of the physical properties as a result of binding. The exploration of molecular electronic depends upon the ability to characterize the physical changes which occur as a result of forming metal-organic interactions. The use of

chemisorption in the exploration of these interactions provides a direct means for the illustration of effects between the adsorption of organic films onto a metal surface.

Even though monolayers can form on a variety of surfaces, the ability to be employed in analysis of surface molecule interactions is considered a necessity. In order to consider a surface for use in molecular studies several parameters must be met. The surface must contain regions that remain consistent through multiple samples. The reproducibility of surfaces provides a methodology in which various experimental avenues of surface effect of molecule interactions are explored. Another aspect of surface characteristics requires that the substrate must possess properties conducive to the analysis of monolayer characteristics with respect to an instrument's operating parameters. Finally, the use of surfaces in characterizing monolayer systems requires surfaces capable of supporting SAMs with low occurrences of defects. To facilitate high order, low defective, monolayers "atomically rough" metals provide surfaces fit for forming these SAMs.

2.2. Faceted Surface

Several approaches exist for fabricating atomically rough surfaces; however, most of which require the use of thermal annealing to create the flattest surfaces possible. In order to create surfaces flat enough to provide a means of analysis with STM, the method of thermal annealing of bulk noble metals was chosen for the creation of faceted surfaces. Thermal annealing allows the generation of faceted surface, which consist of atomically flat terraces as a result of ordering through annealing. Annealing presents the concept that as heat is added to a system, atoms on the surface mobilize to decrease overall surface energy with respect to their surface tension. Afterwards, as the system begins to

cool the atoms on the surface organize into regions of higher order and lower energy. Utilizing annealing on metals relies upon using high purity metals to minimize defects within the terraces and to promote larger facet formation. The creation of faceted surfaces hinges on the concept that forming ordered regions depends upon an endothermic process where the elastic-long range bonding forms ordered boundaries that overcome the intrinsic surface tension.⁶ The elastic-long range bonding formed between atoms within the top few layers of the surface relies upon the addition of bonding energies among each cluster of atoms. As these clusters of atoms interact with other clusters, terraces begin to form from the clusters creating a surface that maintains an orientation respective to that of the clusters. Thus, these interactions create a method of forming atomically flat surfaces used in characterization of surface/interactions.

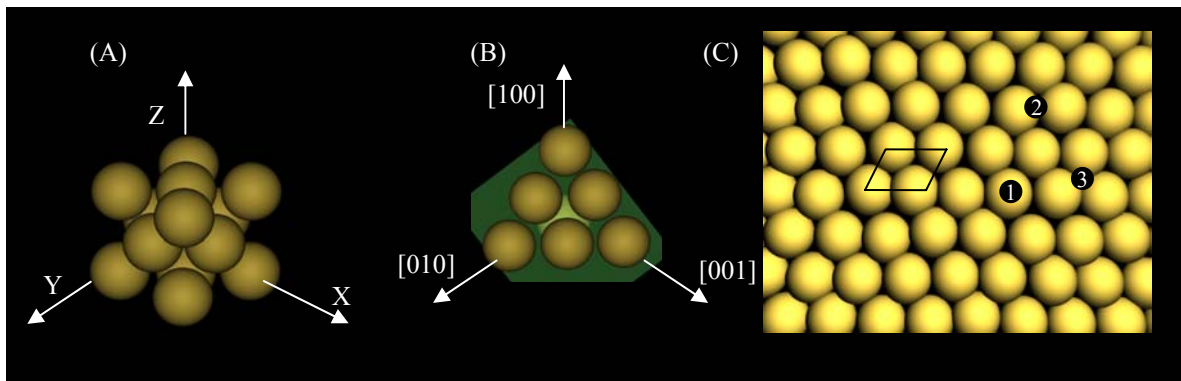


Figure 2.3 a) A representation of a face-centered cubic (fcc) unit cell common to gold, palladium, and platinum. b) A fcc unit cell cut through the $[111]$ axis to illustrate a crystallographic representation of a (111) plane. c) An illustration of (111) lattice structure that uses a $\sqrt{2}/2$ atomic spacing to form a terrace. Sites 1, 2, and 3 represent binding sites which can be characterized by coordinate systems respective to adjoining molecules.

Faceted surfaces consist of atomically flat terraces that possess a specific orientation with respect to crystallographic features. The basic face-centered cubic (fcc) unit cell (Figure 2.3a) represents the normal structure common to that of gold, palladium, and platinum. Through the use of fcc unit cells, it is possible to manipulate the model by

bisecting the [111] axis (Figure 2.3b) creating a plane of orientation. The clusters that possess this orientation combine to create a plane in which atomically flat terraces form (Figure 2.3c). The atomic spacing ratio of $\sqrt{2}/2$ respective to the bond lengths of a given metal allows for the formation of hollow sites that permit the adsorption of molecules onto the surface. There are three types of hollow sites possible within the (111) lattice common for faceted gold illustrated in Figure 2.3c numbers one through three.

Hollow sites are characterized through the use of a coordinate system which depends upon the surface molecules in contact with the adsorbed molecule. For instance, thiols are reported to adsorb to the threefold hollow sites of Au (111) by Balzer et al. through the inspection of the low energy electron diffraction (LEED).⁷

Balzer's group used vapor deposition of alkane thiols in characterizing the adsorption process through formation of monolayers. The purpose of using vapor deposition was to provide an exploration of comparative properties of monolayers formed through the use of ethanol solutions (Figure 2.4). As

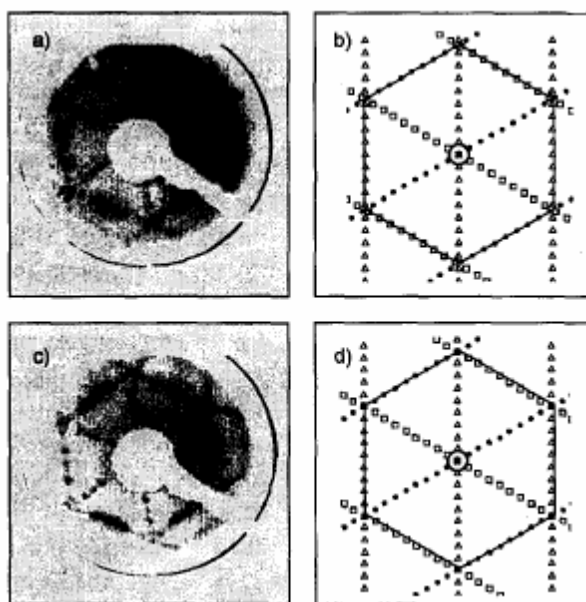
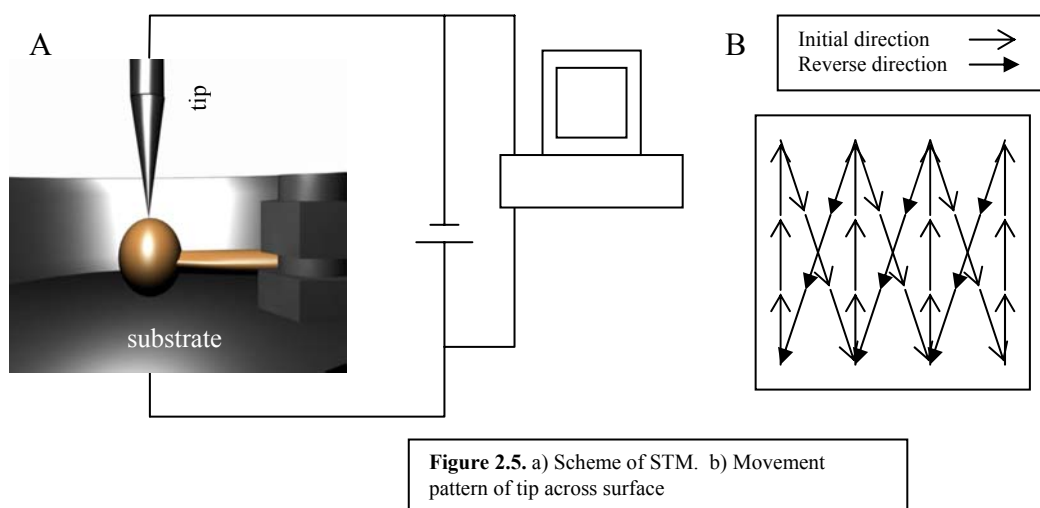


Figure 2.4. (a) LEED pattern obtained for an incident energy of 40 eV for dodecane thiol on Au(111). The surface temperature was 150K. Preparation was via the thermal treatment (430 K) of films that were deposited from ethanolic solution. (b) Calculated LEED pattern, corresponding to a $p(13 \times \sqrt{3})$ structure. The three different symbols (Δ , \bullet , \square) denote three domains rotated by 120° with respect to each other. (c) Same as (a), but for an incident energy of 42.5 eV and the dodecane thiol was vapor deposited at 150 K, heated to 330 K and cooled again to 150 K. (d) Same as (b), but corresponding to a $c(27 \times \sqrt{3})$ structure.⁷

seen with the LEED pattern projections vapor deposition and ethanolic solution deposition provides similar monolayers with domains that rotate by 120° with respect to each other. These domains create patterns atop of the metallic terraces; which also occur upon faceted gold as well. Formation of SAMs on faceted metals provides a means to analyzing properties of the monolayer with respect to the metal surface. To investigate the electrical properties of monolayers formed on faceted surfaces, STM provides measurements that enable the exploration of surface properties.



2.4. Principles of STM

Basic principles in the setup of STMs present an opportunity for the explorations of molecular junctions. STM schemes (Figure 2.5.a) include the utilization of a mechanically cut or electrochemically etched tip, which approaches an electrically charged substrate that may contain a film or monolayer, prepared using various deposition techniques. The resolution capabilities of a STM depend upon the cross-sectional dimensions of the tip and the alignment of the tip relative to the perpendicular plane of the surface and the piezo scanning tube. As the tip scans across the surface in a pattern respective to Figure 2.5.b, the height or conductance of the substrate is illustrated by the creation of an image that projects a three-dimensional perspective of height or

current densities onto a plane through color contrasting. The creation of visual images allows a qualitative characterization of surface features. The establishment of components relevant to the functionality of STM operations provides a deeper understanding to specific attributes significant to the exploration of future paths related to molecular device investigation.

Scanning tunneling microscopy depends upon the quantum principle that the flow of electrons can tunnel through a given material over a confined distance. The process of tunneling in the STM setup is controlled by the relative distance of the tip to the surface commonly referred to as tip height. The distance from the tip to the surface is controlled by two independent features. As the voltage bias applied across the tip and substrate increases from a few millivolts to several volts; the distance increase exponentially between the tip and substrate. The reverse is true for the relationship between current and distance; as distance increases the tunneling current decreases exponentially from several nanoamps to a few picoamps. The distance relationship between the tip and substrate depends upon the potential barrier of the substrate. Therefore, the establishment of the initial height can not be determined. Yet the range in which the tip height changes as it passes over the surface of the sample provides measurable methodology for the characterization of surface dimensions. STM's two electrode system facilitates the regulation of voltages and current through the utilization of complex circuitry.

The use of circuitry to monitor conditions between the two electrode setup precludes the use of a third electrode as a reference. So that the establishment of electrochemical interpretations for STM processes becomes a matter of estimating possible avenues confined to surface chemistry characteristics. In the setup of

electrochemical cells for the reference electrode provides a standardized system for monitoring the application of voltage between electrodes; as well as, the flow of current through the solution. For the majority of STM setups the use of vacuum, air, or solution within the cell provides a medium for tunneling. Solutions in the setup consist of nonpolar solvents such as dodecane. These mediums prevent the employment of a third electrode due to low conductance. However, the lack of a third electrode does not preclude the exploration of surface chemistry.

2.4.1. Molecular approaches to characterizing SAMs

There exist several methodologies for characterizing the formations of monolayers through the use of STM. The measurement of a monolayer's surface structure provides an insight into the orientation and assembly of molecules adsorbed onto the substrate. Also, the measurement of a monolayer's surface structure reveals the ability to effectively pack molecules onto the substrate. In order to fully explore these possible configurations, multiple types of monolayers assembled on gold have been studied.⁸⁻¹¹ Studies of surface characteristic using methods other than STM to identify characteristics of the monolayer that occurs beneath the exposed surface. The utilization of multiple surface characterization experiments present comparable data for monolayer and surface structure; the effect of substrate characteristics on molecular ordering develops as these studies evolve.

In the process of analyzing surface dependent effects observing the state of the surface without perturbing its structural characteristics was paramount. To facilitate a discrete study, the scanning parameters of the STM cannot exceed potential values that

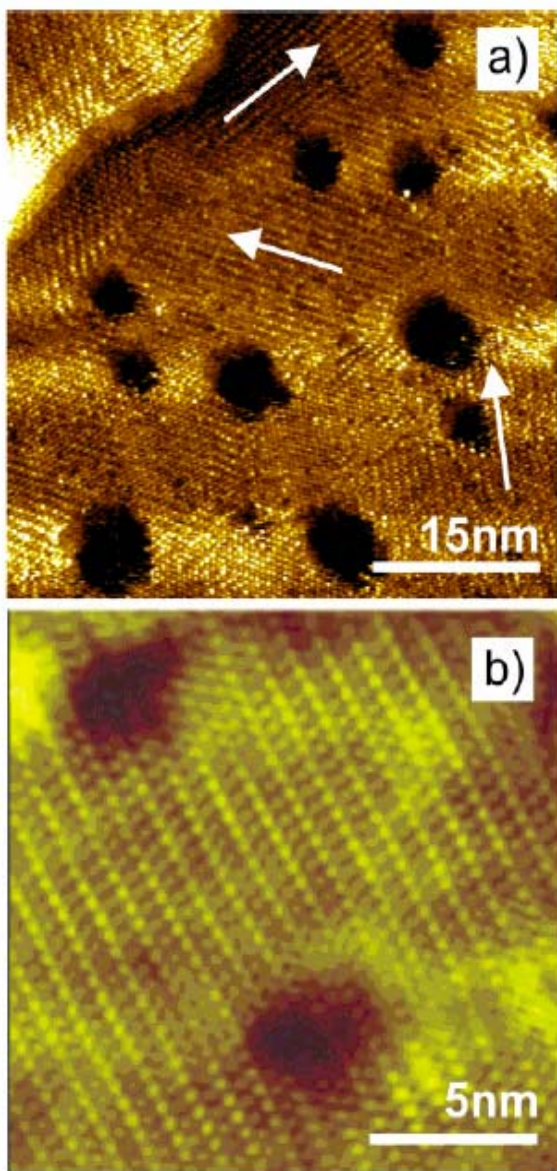


Figure 2.6. Constant-current images for a Au(111) substrate, which has been immersed for 24 h into a 100 μ M solution of BP3 in ethanol at 333 K. Three different rotational domains corresponding to the Au(111) substrate symmetry are indicated by arrows. An enlarged image demonstrating molecular resolution is shown in panel b. Tunneling parameters: (a) U 1 V, I 600 pA; (b) U 0.59 V, I 110 pA.⁸

would destroy the surface. Azzam et al. presented an investigation of ω -(4'-methylbiphenyl-4-yl) alkanethiols, later referred to as BP3 or BP4 depending on length of alkane chain respectively. Relying on STM and LEED to characterize possible explanations of adsorption interactions and structural orientation as seen in Figure 2.6.a.⁸ The establishment of structural orientation of BP3 via molecular resolution image provides insight into the effect of sterics on the thiolate binding to the substrate. Upon presenting a comparison of BP3's structural characteristic to that of alkane thiolate monolayers Azzam's group discovered through STM and LEED measurements that little tilt variations occurs as a result of the

phenyl ring and that the threefold hollow site observed in alkane thiolate also occurred in BP3 monolayers.⁸ On the other hand, when comparing BP4 monolayers, the adsorption sites were not specified due to a high number of diffraction sites. In comparing structural characteristics of biphenyl monolayer, methodologies were developed to establish the effects of molecular structure on adsorption.

The formation of monolayers depended on several characteristics of molecular structure. The Gorman's group investigated the effects of headgroup variation on monolayer formation. Headgroups were referred to as the terminated ends of adsorbed molecules which form domains with specific surface characteristics. For instance in Gorman's et al. exploration used STM imaging of alkene, cyano, and carboxylic acid terminated thiols to provide comparative results to that of methyl terminated thiols of similar length on Au (111) surfaces.¹¹ Through utilization of molecular imaging the illustration of headgroups and environmental effects on ordering became comparable as a result of measuring the distance between molecules of the adlayer. Analysis of alkene and methyl functional groups demonstrated that SAMs composed of similar size functional groups formed structures of comparable dimensions.¹¹ The investigation of cyano and carboxylic acid groups revealed the ability of alter surface properties, as well as, surface structure through the alteration of environmental conditions. The use of relative humidity to limit the hydrolysis of cyano groups into amido- or carboxylic acid SAMs showed a technique to creating a chemically specified monolayer. The study of cyano- terminated thiols relied upon monitoring the alterations within the adlayer conveyed within the regions of varied orientations. While undecane-1-thiol monolayer possessed an orientation of 120°, 10-cyanodecanethiol monolayers have unit cell

orientations of 105° and 90° demonstrating similar results to that of mercaptoundecanol, cysteamine, and mercaptoundecylamine SAMs that utilize hydrogen bonding in the ordering of the monolayers.¹¹ The investigation of SAMs relies on the ability to analyze the structural characteristics of the monolayer; which can be based on high resolution analysis of surface molecules.

2.5. Conclusions

The exploration of surface science requires establishing a set of techniques for the preparation of surfaces. Preparation of surfaces capable of presenting characteristics of molecular structure requires the ability to create well packed, consistent SAMs. The fabrication of SAMs for STM relies on the use of atomically flat faceted surfaces. The use of STM in molecular studies consists of the ability to investigate the ordering of SAMs; as well as, electrochemical aspects that govern the adsorption and desorption processes within the monolayer. The inspection of electrochemical processes within monolayers can be explored using STM with replacement lithography; which is encompassed in the studies of substrate variation.

2.6. References

- (1) H. Sakuma, M. Iizuka, M. Nakamura, K. Kudo. *Thin Solid Films* 438 –439 (2003) 326–329.
- (2) O. Dannenberger, K. Weiss, H.-J. Himmel, B. Jäger, M. Buck, Ch. Wöll. *Thin Solid Films* 307 (1997) 183-191.
- (3) R. Gerlach, G. Polanski, H.-G. Rubahn. *Thin Solid Films* 318 (1998) 270-272.
- (4) A. Ulman et al. *Reviews in Molecular Biotechnology* 74 (2000) 175-188.
- (5) D. Vuillaume, S. Lenfant. *Microelectronic Engineering* 70 (2003) 539-550.
- (6) V. Shchukin, D. Bimberg. *Rev. of Mod. Phys.* 71 (1999) 1125-1171.
- (7) F. Balzer, R. Gerlach, G. Polanski, H.-G. Rubahn. *Chemical Physics Letters* 274 (1997) 145-151.
- (8) W. Azzam, P. Cyganik, G. Witte, M. Buck, Ch. Wöll. *Langmuir* 19 (2003) 8262-8270.
- (9) Shu-Yi Lin et al. *J. Phys. Chem. B* 108 (2004) 959-964.
- (10) Woo Lee. *Langmuir* 20 (2004) 287-290.
- (11) C. B. Gorman, Y. He, R. L. Carroll. *Langmuir* 17 (2001) 5324-5328.

Chapter III

Replacement Lithography

3. Replacement Lithography

A percept of lithography relies on minimizing fabricated dimensions upon a surface. Exploiting lithographic techniques to characterize surface interactions presents avenues for the development of structural features that adhere to electronic philosophies. The implications of designing structural features with an electronic purpose provide insight into the future development of molecular scale devices. Expounding further upon this notion, requires decreasing the scale of structures while maintaining their electrical potential. Thus scaling down requires the employment of single/multi-molecule systems. Exploring interactions using a two electrode system with an atomically confined region demands the use of lithographic techniques, such as replacement lithography. Replacement lithography (RL) operates through the implementation of potentially driven

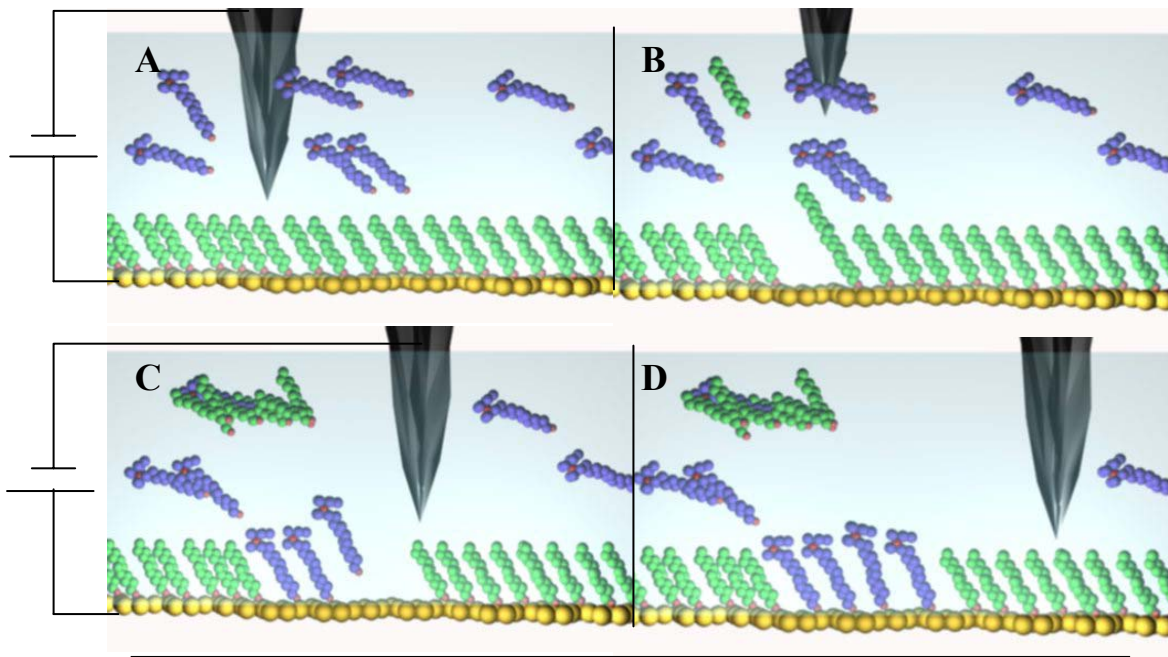


Figure 3.1. (A) Initial scanning setting designed to observe SAMs without perturbing the monolayer. (B) Desorption of the monolayer into solution as a result an increase in applied potential. (C) Replacement of the monolayer with substituted molecules into desorption sites. (D) Return to initial scanning parameters.

desorption. Figure 3.1 presents an illustration of the process that allows RL to characterize various aspects of molecular structure. The initial scanning parameters demonstrate the possible possibilities of examining features of surface structure without perturbing the arrangements of adsorbed molecules seen in Figure 3.1.A. Thus, initial scans provide a means of selecting regions on the surface, which presents advantages to further the study of RL. Imaging the surface prior to replacement generates an investigation of initial surface characteristics. Also, RL uses potentially driven desorption to cause removal of bound molecules without destruction or deformation of the substrate (Figure 3.1.B). Studies in which molecules are desorbed from a surface are characterized through the use of analyzing the surface changes before and after desorption or by having molecules, with characteristics that differ with respect to the sample-able parameters of the instrument, adsorb onto the unoccupied surface.¹⁻⁴ Utilizing the insertion of molecules into vacant regions distinguishes the replaced regions from the background monolayer (Figure 3.1.C). Making a distinction of replaced regions relies on the attenuation of tunneling current to highlight the desorbed area. Hence, the effectiveness of RL relies on the ability to distinguish the adsorbed (substituted) molecules from their surrounding. Species capable of having a tunneling current greater than that of background monolayer are of interest when using desorptive lithographic techniques.

Gorman's et al. use of 11-Ferrocenylundecanethiol ($\text{Fc-C}_{11}\text{SH}$) and phenoxygalvinol-substituted hexanethioacetate ($\text{Gal-C}_6\text{SH}$) replaced into a dodecanethiolate SAM on Au (111) surface illustrates a possible avenues for characterizing desorptive potentials through the use of scanning probe lithography

(SPL).¹ Their examination of these replacing molecules employed a comparison of the resulting apparent height contrast (i.e. the average measured height difference between monolayer and replaced molecules at given parameters). In comparing (Fc-C₁₁SH) and (Gal-C₆SH), the application of various potential scanning biases revealed that the inherent apparent height contrast reaches a threshold and proceeds to increase with applied bias (Figure 3.2). (Gal-C₆SH) yielded a greater height contrast at lower biases than Fc-C₁₁SH presenting a qualitative measurement of distinguishing electroactive molecules adsorbed into the SAM, a non-electroactive background. Thus, the apparent height contrast based on variations of imaging biases present descriptive characteristics of the potential bias's effect on the relative tunneling conductance within molecules. The lighter regions of the image indicate a greater distance between tip and molecule. In order to maintain constant current and bias potential, the distance must increase to minimize molecular conductive effects on potential tip states.

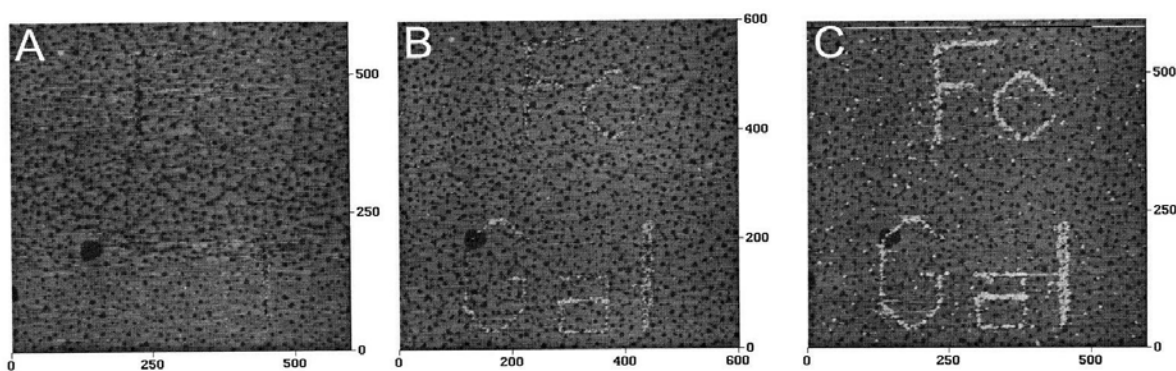


Figure 3.2 Apparent height difference of electroactive thiols at varying imaging biases under dodecane. The letters “Fc” were written with Fc-C₁₁SH, and the letters “Gal” were written with Gal-C₆SH. RC: 3.0 V, 10 pA, 50 nm/s; RH, 59%. IC: 600x600 nm, 3 nm z scale, 10 pA, 1 Hz scan rate. Imaging bias: (A) 115 mV, (B) 700 mV, and (C) 1800 mV¹.

3.1. Causes of Variations

Replacement Lithography utilizes the narrow dimensions of the STM tip to produce lithographic dimensions between 5-25 nm in width. However, producing consistent dimensional characteristics depend on several mitigating factors. Tips used to potentially cause desorption of molecules within a monolayer are produced in several fashions. The use of mechanically cut or chemically etched tips provides a variety of technical variations to the formation of “atomically” sharp tips. In order to maintain consistency, RL experiments are conducted with each tip and only those that produce dimensional widths between 5 nm and 15 nm are accepted. However, the tunnel junction at the end of the tip does not exclusively control variation. The initial position of the tip over the monolayer relative to regions of order influences the overall completeness of replacement. For instance, initially beginning desorption within a disordered region allows a lower potential window to achieve relatively high percentages of replacement; resulting from lower stabilities attributed to disordered regions. Another problematic variation provided by regions of disorder and defect sites corresponds with adventitious replacement of substituting molecules.

Impeding the rate of adventitious replacement allows for images with clearly defined substituted regions. Adventitious replacement depends on the thickness of the monolayer, amount of disordered regions, relative humidity, affinity of terminal groups for the surface, and concentration of substituted molecules. In order to limit the rate of adventitious replacement, the thickness of the monolayer and the relative size and stability of the terminal group act as a steric barrier to potential binding sites. Also, the stability of lower ordered regions on the surface cause a general variation in the relative

affinity of the monolayer compared to that of the substituted terminal groups. These implications infer that molecules of the monolayer may exchange with replacing molecules that are in higher concentrations and have similar or greater affinity for the substrate. Inhibiting unwanted exchange relies on the use of terminal groups with a lower affinity for substrates used in experimentation. Facilitating RL experiments depends on controlling the concentration of the substituting molecules so that the propagation of adventitious replacement remains minimal, but the concentration must be high enough that replacement still takes place. The employment of thioacetate instead of thiol terminated molecules for RL illustrates the use of both steric limitations to binding sites as well as molecules with a lower affinity for substrate. Finally, relative humidity plays several roles within RL. Humidity is used in controlling adventitious replacement and replacement of desired regions. While the mechanism in which relative humidity regulates replacement is unknown, the predominate interpretation uses a thin water layer, which forms on the surface of the monolayer collected from the moisture in the air. The water thickness and composition of the water layer have yet to be investigated, however a correlation between the ability to acquire molecular resolution imaging and humidity suggest that the water layer at the surface-tip interface distorts tunneling consistency based on the SAMs properties.⁵ A common parameter for relative humidity when investigating RL ranges from 53%-57%, while other lithographic techniques use lower relative humidity.⁶⁻⁸ Yet, many variations which occur are dependent on substrate characteristics.

3.2 Various Substrates

The investigation of substrate dependent phenomena requires an examination of several aspects of that effect the metal/molecule interaction through the use of multiple experimentations. In performing substrate dependent experimentation, the establishment of consistent surfaces preparation and characterization is a necessity. The ability to prepare a surface depends on properties of the metals chosen for substrates. Initial substrate based experiments were intended to encompass copper, silver, gold, platinum, palladium, and zinc substrates. However upon attempting to anneal copper, silver, and zinc, it was found that oxide layers quickly formed along the surface preventing the formation of facets. Even when these metals were flame annealed in an atmosphere lacking high concentrations of oxygen, a low density oxide layer still engulfed the surface. To this end only substrates of gold, platinum, palladium (Figure 3.3) were prepared and studied with replacement lithography to characterize surface interactions as explained in section 3.2.1.

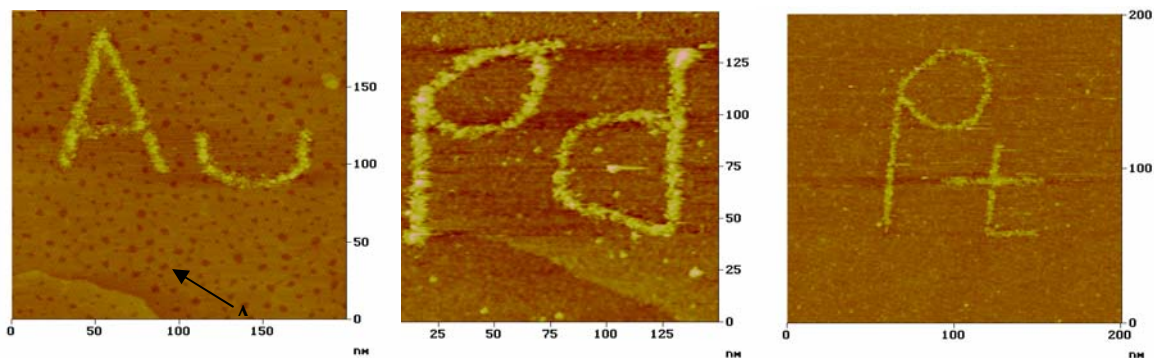


Figure 3.3 Images of replacement lithography labeled with respect to perspective substrate metal and replacing molecule is (Fc-C₁₁SAc) into dodecanethiolate monolayer. Imaging conditions: Au and Pd 1.7 V scan bias, 10pA, and 3nm Z range; Pt 1.9V scan bias, 10pA, and 3 nm Z range. RL conditions: ~55% relative humidity and biases of 3.4V, 3.1V, 3.55V respectively written at 20nm/s within replace regions. A) Pit region within the monolayer surrounded by visible lines called domain boundaries.

3.2.1. Surface Characteristics

Upon comparison of surface structures on gold, platinum, and palladium, an initial conceptualization of variations between surfaces developed. In spite of a lack in previously established precedent involving SAMs formed on platinum and palladium surfaces. Examination of gold surfaces reveals the formation of pits and domain boundaries denoted by Figure 3.3.A. Pit regions reflected the removal of a single gold atom layer within the darkened region by the thiolate during the formation of the monolayer. A feasible explanation for this phenomenon related the removal of the gold atom layer occurs as a result of chemisorption-induced vacancy islanding while attempting to lower the surface free energy of the monolayer.⁹ The darkened lines connecting the pitted areas represent domain boundaries that formed between the rotational axis of the thiolate lattices. Upon examining the surfaces of palladium and platinum thiolate monolayers no pits or domain boundaries were visible, suggesting the possibility that lower surface coverage prevents formation of pits and domain boundaries. To further the study of various substrates RL experiments were conducted on each of the metals revealing the effects of surface-molecule interface.

In comparing the efficacy of replacement based on the percentage of replacement, the over all trend indicates whether or not the adherence to potentially driven desorption provides a consistent measure of substrate-monolayer interactions (Figure 3.4). Also, the approximation of error in sampling allowed the observed of voltages to indicate the respective threshold efficacy of the substrate. Threshold efficacy referred to the potential of applied bias in which the molecule most efficiently desorbed from the surface at a given writing rate and monolayer composition. Monolayer composition consisted of the

adsorbed molecules, as well as, the affinity that replacing molecules had for the surface. For instance, by simply changing the monolayers respective height through the use of different alkane chain lengths, the potential threshold to desorb molecules was decreases with the respective length of the molecule analogous to equivalent electrochemical experimentation.¹⁰ Also as presented in Section 3.2.2 the formation of oxides on the surface can dramatically affect the replacement threshold. As far as the control of the substituting molecules' affinity to bind to the surface, drastic changes in threshold potentials can occur caused by low humidity which shifts the desorption threshold. Further examination of replacement images seen in Figure 3.4 illustrates that replacement potentials fail to provide an exact potential that correlates directly to the beginning of desorption. Thus, RL presents itself as being indicative of a system to characterize

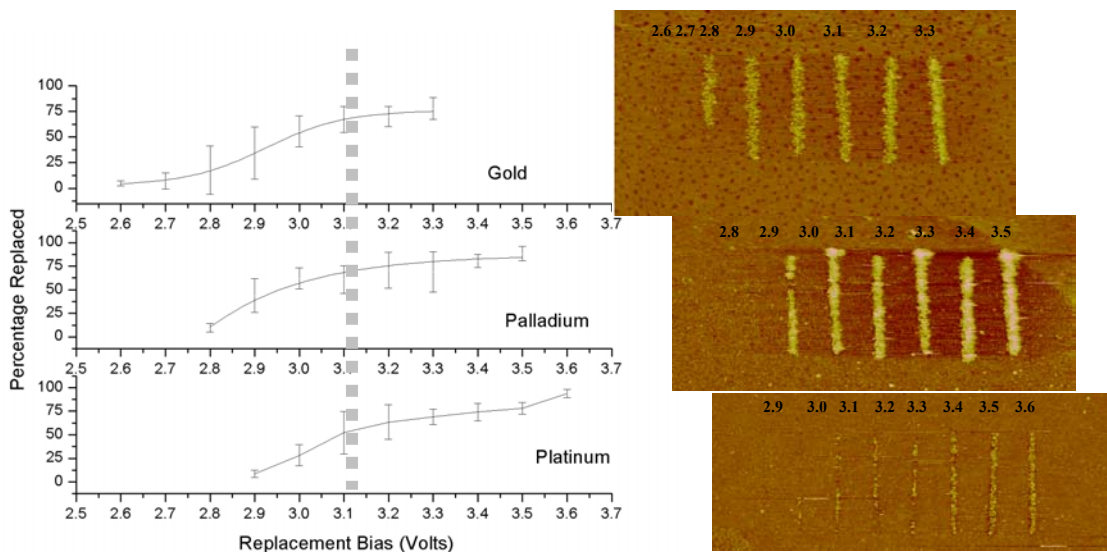


Figure 3.4 A graphic representation of the Percentage of Fc-C₁₁Sac Replacement versus Replacement Bias (the lines are meant to guide the eye through mean percentage of each bias). Adjacent images represent data points for the graph with lines generated as a result of Voltage biases listed above each line with respective substrate indicated by adjacent labeled graph. Gold, platinum, and palladium substrate imaging conditions $V_{\text{bias}}=1.7\text{V}$ scale= 350nm^2 , $V_{\text{bias}}=1.9\text{V}$ scale= 400nm^2 , $V_{\text{bias}}=1.7\text{V}$ scale= 350nm^2 respectively. All setpoint and Z-scale were 10pA and 3nm.

changes in surfaces as well as ordering and stability of the monolayer. However many factors dictated the overall success inherent to the replacement process.

The interpretation of surface characteristics in relation to the work functions of the metals allows an explanation of the shift in the threshold when comparing substrates. As seen in Figure 3.4, trends for gold, palladium, and platinum monolayers desorb in the same order as the increasing work functions for (111) orientations of respective metals (Table 3.1). Also, a comparison of work functions made with platinum's potential difference between the respective work functions of gold and palladium implies that the higher magnitude of platinum's work function indicates that the threshold of replacement should be shifted higher than that of palladium or

gold. As shown in Figure 3.4, the average percentage of replacement barely approaches 85% until reaching 3.6V replacement bias. Hence, the

	Macroscopic	
Surface	Work Function	Fermi level
Au(111)	5.68	6.72
Pd(111)	5.95	6.47
Pt(111)	6.40	5.90

Table 3.1. List of work functions with respect to substrate and orientation.¹¹

proportionally higher work function of platinum would indicate that replacement lithographic experiments based on substrate variation depends on the ability to reduce the bound molecule to facilitate desorption. Since, higher work functions are synonymous with the energy required to remove electrons from the substrate, then as work function increases so does the threshold potential.

3.2.2. Effect of Surface Oxides

The principles of replacement lithography operate on the basis that minute changes in preparation can have a dramatic impact on the stability and characteristics of the monolayer. All preparatory procedures were adhered to and specifically design to minimize adventitious replacement and produce consistent SAMs. To this effect, when

preparing, a thiolate monolayer on platinum or palladium etching solutions of concentrated sulfuric acid, in a 1:3 ratio of distilled water and concentrated sulfuric acid respectively were used to minimize oxidation. However due to a lack of prior established available knowledge in the preparation of thiolate monolayers on platinum or palladium, samples were simply annealed in a $H_{2(g)}/O_{2(g)}$ flame. Thus the lack of etching allowed for a thin film of oxide to form in scattered regions across the facet. Palladium in particular suffered from large oxide regions (Figure 3.5.A) that appear in similar shape

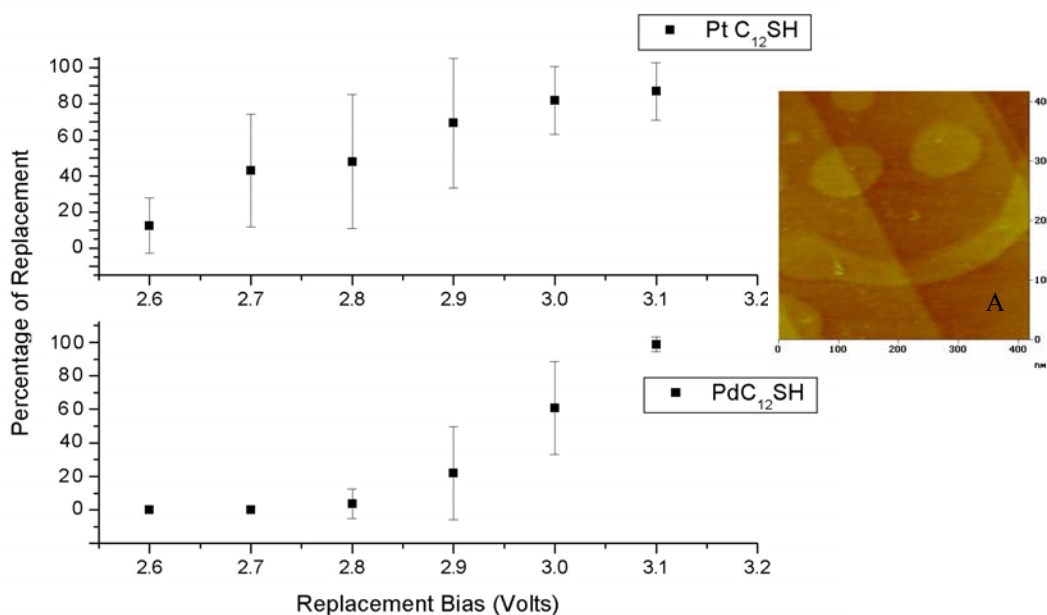


Figure 3.5 Graphs of Percentage of Fc-C₁₁SAc Replacement versus Replacement Bias of un-etched platinum and palladium. A) Pd C₁₂S monolayer imaged at 1.0V, setpoint 10pA, scan size 400 nm², and 3nm Z-scale.

and size throughout the surface, indicating islanding of oxides on the surface. When comparing the results of Figures 3.4 and 3.5, the trends obviously denote the instability of the surfaces prepared without etching as seen in the large errors in reproducibility. Palladium in particular demonstrates an alteration of surface characteristics shown by the sudden increase in the percentages of replacement. Thus the effect of oxides on metals

such as platinum and palladium reveal a potential source of error when exploring their surface characteristics without the proper preparation of the substrates.

3.3.3. Transconductance

Transconductance provides the ideal means for carrying out replacement lithography with a STM. Through the applications of various potentials as seen previously in Figure 3.2, transconductance allows a varying amount of tunneling current to pass through the molecule at a given resistance. As the Fermi level of the tip aligns with that of the molecule, the conductance of the molecule increases causing brighter regions to appear. In order to obtain the greatest response, a series of scan biases over a replaced region were compared revealing the optimal scan bias for each of the substrates used in RL experiments. Also, shifts in optimal bias scans seen in Figure 3.6 show that 1.7 V for gold monolayers, 1.7 V for palladium, and 1.9 V for platinum agreed with the trend of Fermi level projected in Table 3.1. Thus, transconductive trends provide another method of characterizing substrate interactions with bound molecules.

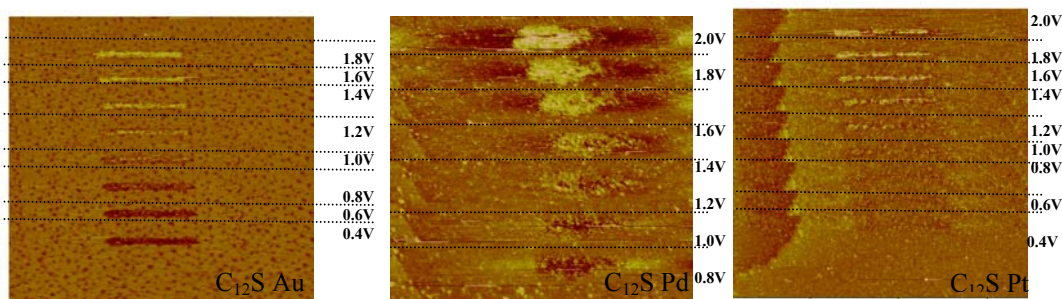


Figure 3.6 Above images reveal the effect of varying applied bias on the replaced molecule (Fc-C₁₁S) on various substrates labeled in bottom right of each images with scan bias listed to the right with respect to

3.4. Conclusions

In utilizing replacement lithography to characterize various aspects of the substrate-molecule interface, a relationship between desorption potentials and work functions was established. RL also revealed the effect of oxidation on surfaces prior to the adsorption of a monolayer, which causes shifts in the potential required to desorb molecules from the surface. As well as presenting inconsistency in replacement attributed to a mixed oxidized surface seen by the vast variation in replacement percentages, which was inferred from the reduced accuracy of verifying threshold potential. The observations based on the transconductance of Fc-C₁₁S revealed potential shifting in I-V characteristics resulting from variations in Fermi levels of chosen substrates. However in spite of numerous studies the lack of a third electrode as a reference presented the need for reductive desorption experimentation based on an electrochemical setup. Yet, in order to equate potential scans from an electrochemical setup, a more in depth explanation of monolayer bulk characteristics must be explored.

3.5. Experimental Design

3.5.1. Fabrication of Substrates and Preparation of Monolayer

Substrates were obtained from Alfa Aesar and prepared from 0.5mm diameter Au(99.999%), Pt(99.99%), and Pd(99.99+%). Thiol solutions were created using n-dodecane thiol (98%) and diluted to 1.0mM in ethanol. Gold substrates were prepared as following: 0.5mm diameter wire was attached using H_{2(g)} flame to a platinum disc cut from 25mm thick Pt foil (99.99+%) obtained from Alfa Aesar. The end of the gold wire was then annealed using a H_{2(g)} into a ball, which was then purified through continuous

annealing of the sample. To clean the surface from impurities, samples were placed in freshly prepared piranha composed of 1:3 30% H_2O_2 and H_2SO_4 respectively. Finally, gold samples were then reannealed and placed in the thiol solution followed by refluxing for one hour at $\sim 120^\circ\text{C}$, with an hour of incubation afterwards. Platinum substrates were prepared by annealing one end of the wire in a $\text{H}_{2(\text{g})}/\text{O}_{2(\text{g})}$ flame to a purity high enough to form facets along the surface. Once a facet on the surface was selected, the remaining wire was bent to prevent damage to the facet from annealing. Then, the sample was etched in concentrated sulfuric acid for 15 minutes. After which the samples were rinsed extensively with distilled water and absolute ethanol then immersed in the thiol solution. The samples were then refluxed for one hour, incubated for 24 hours, and refluxed for an additional hour. Palladium samples were prepared in the same fashion as platinum samples, except the $\text{H}_2/\text{O}_{2(\text{g})}$ flame contained only trace amounts of $\text{O}_{2(\text{g})}$ to minimize oxidation and overheating. Also, the etching solution consisted of a 1:3 ratio of distilled water and concentrated sulfuric acid respectively, and the final reflux was skipped. Upon completion of sample preparation, the samples were then rinsed with ethanol and blown dry with $\text{N}_{2(\text{g})}$. Finally, samples were aligned in the STM cell and replacement experiments were conducted.

3.5.2. Procedure for Replacement Lithography

STM images were obtained using a mechanically cut tip of 90:10 Pt:Ir 0.25mm diameter annealed wire from Alfa Aesar. Images were obtained using Nanoscope III scanner purchased from Digital Instrument. Samples placed in the STM were immersed in $\sim 350\mu\text{L}$ of dodecane obtained from Fisher with $25\mu\text{L}$ of 11-ferrocenylundecanethioacetate diluted to 0.1mM in dodecane. The relative humidity of

the atmosphere within the STM was adjusted to ~55% over the course of two hours by bubbling N_{2(g)} through distilled water. Replacement lithographic programs were run to facilitate replacement at 0.1 increasing increments in voltage scanning bias. Afterwards the surface was scanned at a high enough bias to maximize the transconductance of the electroactive ferrocene molecule replaced into the region. The images obtained from these experiments were thresholded using Scion Image. The length and width of the highest bias replaced region were measured and used to calculate the maximum theoretical area of replacement. Afterward each of the replaced regions were measured and the ratio with respect to maximum replaced region was established yielding percentage of replacement. A biased based graph for each metal versus percentage of replacement was composed to demonstrate effects of metal on replacement.

3.6. Programs

3.6.2. Variation of Voltage

```
#include <litho.h>

void main()
{
LITHO_BEGIN

double startvoltage = 2.5; //voltage of first line etch
double r=0.02; // writing rate
double u=5*r; //time for lime to write
double f=-0.0001; //drift compensator
double scan= 1.0; //voltage between scans
double wide=0.035; //distance between scans
double d=-u;
double increment = 0.1; //increment of voltage
double rate = 0.02; //move tip in x-y at this rate in um/s

LithoTranslate ((-(3*wide)-.035), 0, rate); //move to starting point
LithoTranslate (0, 0.01, rate);
LithoTranslate (0, -0.01, r);
LithoSetOutput (aoBias, startvoltage); // turn on at startvoltage
LithoTranslate ( 0, u, r);
LithoSetOutput (aoBias, scan); //turn off
LithoTranslate ( wide, 0, rate); // move
LithoSetOutput (aoBias, startvoltage+1*increment); // turn on and etch
```

```

LithoTranslate ( 0, d, r);
LithoSetOutput ( aoBias, scan); // turn off
LithoTranslate ( wide, 0, rate); // move
LithoSetOutput (aoBias, startvoltage+2*increment); // turn on and etch
LithoTranslate ( 0, u, r);
LithoSetOutput ( aoBias, scan); // turn off
LithoTranslate ( wide, 0, rate); // move
LithoSetOutput (aoBias, startvoltage+3*increment); // turn on and etch
LithoTranslate ( 0, d, r);
LithoSetOutput ( aoBias, scan); // turn off
LithoTranslate ( wide, 0, rate); // move
LithoSetOutput (aoBias, startvoltage+4*increment); // turn on and etch
LithoTranslate ( 0, u, r);
LithoSetOutput ( aoBias, scan); // turn off
LithoTranslate ( wide, 0, rate); // move
LithoSetOutput (aoBias, startvoltage+5*increment); // turn on and etch
LithoTranslate ( 0, d, r);
LithoSetOutput ( aoBias, scan); // turn off
LithoTranslate ( wide, 0, rate); // move
LithoSetOutput (aoBias, startvoltage+6*increment); // turn on and etch
LithoTranslate ( 0, u, r);
LithoSetOutput ( aoBias, scan); // turn off
LithoTranslate ( wide, 0, rate); // move
LithoSetOutput (aoBias, startvoltage+7*increment); // turn on and etch
LithoTranslate ( 0, d, r);
LithoSetOutput ( aoBias, scan); // turn off

LithoTranslate ( f, 0.0, 2*rate); // drift corrections
LithoSetOutput ( aoBias, scan); // turn off
LITHO_END}

```

3.6.3. Variation of Scanning Bias for Transconductance

```

#include <litho.h>
void main()
{
LITHO_BEGIN
double rate=0.02;
double bias=3.1;
LithoSetOutput(aoBias,1.0);
LithoTranslate (-.045,.15,rate);
//write 1
LithoSetOutput(aoBias, bias);
LithoTranslate (.1,0,rate);
LithoSetOutput(aoBias,1.0);
LithoTranslate (0,-0.05,rate);
LithoSetOutput(aoBias,1.0);
LithoTranslate (0,-0.05,rate);

LITHO_END}

```

3.7 References

- (1) C. Gorman, L. Carroll, R. Fuierer. Langmuir 17 (2001) 6923-6930.
- (2) J. Zhao, K. Uosaki. Langmuir 17 (2001) 7784-7788.
- (3) P. Schwartz. Langmuir 17 (2001) 5971-5977.
- (4) D. Wouters, U. Schubert. Langmuir 19 (2003) 9033-9038.
- (5) C. B. Gorman, Y. He, R. L. Carroll. Langmuir 17 (2001) 5324-5328.
- (6) H. Zhang, Sung-Wook Chung, and C. A. Mirkin Nano Letters 3 (2003) 43-45
- (7) Y. Li, B. Maynor, J. Liu. Langmuir 17 (2001) 2575-2578.
- (8) J. Zhao and K. Uosaki. Nano Letters 2 (2002) 137-140.
- (9) M. Kawasaki, T. Sato, T. Tanaka, K. Takao. Langmuir 16 (2000) 1719-1728.
- (10) T. Kakiuchi, H. Usui, D. Hobara, M. Yamamoto. Langmuir 18 (2002) 5231-5238.
- (11) Hua Zhong, CEM 924 Final Report, April 27, 2001

Chapter IV

Study of Reductive Desorption

4. Electrochemical Adsorption & Desorption

The basic electrochemical setup monitors the state of monolayers that form on a substrate through the use of a three electrode system. Three electrode systems require a reference, working, and counter electrode placed in an electrolyte based solution. The reference electrode samples the potential applied across the working and counter electrode through comparison to an electrochemical standard solution isolated from direct interaction with the electrolyte solution. The purpose of the counter electrode is simply to supply a source to accept or donate electrons into the setup depending on the potential applied across the system. The working electrode supplies a confined surface area that allows the adsorption and desorption of molecules based on their affinity for the metal electrode under investigation. Also, unlike STM which uses tunneling current to control relative distance measurements between tip and monolayer, electrochemistry uses solutions consisting of electrolytes and molecules of interest to study the passage of current between working and counter electrodes. Thus, allowing the concentration of electrolytes in solution and surface area of the working electrode to control the flow of current based on applied voltages. The attenuation in signal ratios current provides a measurement of electroactive species or states of adsorbed molecules on the surface of the electrode. Application of voltages across electrodes controls the rates of adsorption and desorption of monolayer forming molecules. Thus using electrochemical desorption allows the exploration of stability concepts for molecular electronics through the utilization of bulk surface characteristics.



Electrochemical control of the formation and removal of monolayers on a substrate requires the application of voltage potentials. The application of voltage potentials creates a measurable influence of the states of molecules on the surface of the electrode by causing their reductive desorption or oxidative adsorption. The process of reductive desorption consists of the single electron reduction of an adsorbed species on the substrate. Then the reduced species desorbs from the surface creating and increase in current as the concentration of solution to adsorbed molecules change. However the rates of adsorption and desorption depend on several mitigating factors, the affinity of the molecule for the substrate based on the potential applied across system and the type of binding occurring between molecule and substrate. The affinity that molecules have for the substrate is based on its ability to adsorb onto and desorb off of the substrate and the effect that applied potential has. Depending on the method of binding whether chemisorption or physisorption, the rate of desorption varies with respect to applied potential. Primarily studies that rely on the chemisorption of the SAMs for the characterization of non-electroactive monolayers present reductive desorption potential as an explanation of reaction(1). Thus, allowing studies of rates of desorption and adsorption to utilize the variations in formation factors, in order to characterize the fabrication of monolayers and their stabilities.

4.1. Desorption of Alkane thiols on gold

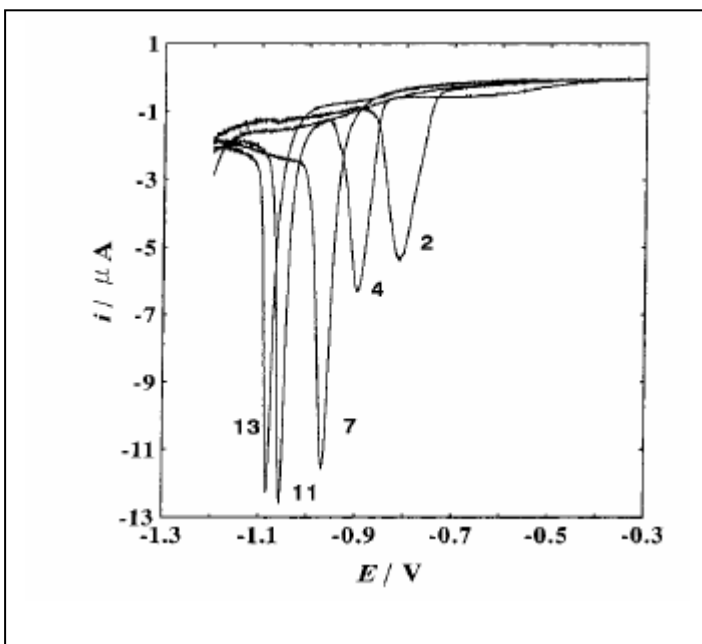


Figure 4.1. Cyclic voltammograms for reductive desorption of self-assembled monolayers composed of alkanethiols recorded with a scan rate of 20 mV/s in 0.5mol dm^{-3} KOH. The number of methylene units is indicated by each curve. Curves are for annealed SAMs except for curve 4.¹

The investigation of reductive desorption alkane thiol monolayers of various lengths provided an extensive background to exploring the effects of substrate variation on desorption potential. Reductive desorption on gold substrates presents a well characterized system in creating an analogous approach to functionalized effects of SAM structure.

Several studies utilized gold's ability to form extremely flat surfaces and to bind effectively creating well order SAMs for reductive desorption experiments.¹⁻³ As seen in Figure 4.1 the desorption potentials of alkanethiols on gold followed a linear increase with respect to the number of methylene units contained in adsorbed molecules when comparing their respective Cyclic Voltammograms.¹ Electrochemical characterization of SAMs relied on the ability to reproducibly form monolayers of consistent ordering and substrates with similar surface properties. Achieving consistent monolayers required the precise regulation of annealing temperatures of SAMs and substrates. The minimization of factors that hinder the formation of SAMs such as surface oxides were required to

explore properties of thiolate desorption.³ Once reliable monolayers are available for study, the comparison between chain lengths on effective desorption potential revealed a shift of -20mV per methylene group at 100mVs⁻¹.¹ With the establishment of a specific shift in desorption potential based on the number of methylene units, the exploration of various substrates through the use of reductive desorption become feasible.

4.2. Electrochemistry of Electroactive Molecules Platinum and Gold Substrates

In order to establish a relationship between various substrates and the chemisorption of species on a surface, the use of electroactive molecules provides a method to probe variations in substrate properties. A methodology to monitoring the adsorption rate of molecules onto a surface utilizes a potentially driven deposition technique to establish the point of zero charge, E_{zero} .⁴ The point of zero charge represents the relative surface charge required to neither inhibit or promote the adsorption of charged species onto the surface. Thus E_{zero} provides a measurement of substrate interactions relative to that of the adsorbed molecules.

Bretz and Abruña used the deposition of $[\text{Os}(\text{byp})_2\text{Cl}(\text{Py}-(\text{CH}_2)_n\text{SH})(\text{PF}_6)]$, of various chain lengths, n , in order to monitor substrate's effect on the E_{zero} . In their exploration of electrochemical adsorption, variation in the potentials of deposition with respect to E_{zero} allowed for the observation of interactions between adsorbed species and those near the surface of the monolayer. Bertz group found that the E_{zero} for platinum substrates were a factor of 4 more positive than those of gold.⁴ After establishing points of zero charge and varying potentials on either side during deposition time, an comparison of substrates revealed that the adsorption of molecules onto the substrate relied on electrostatic interactions to regulate rates of adsorption. Electrostatic control of

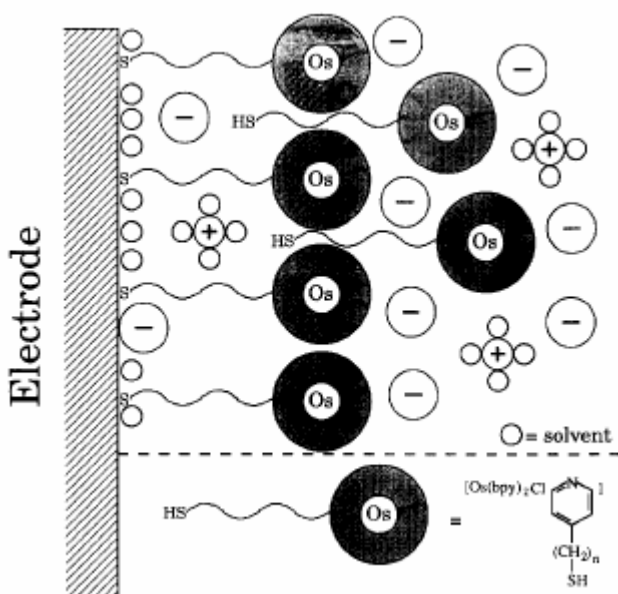


Figure 4.2. Schematic depiction of electrode surface modified by with an osmium thiol monolayer .⁴

attenuation resulting from the electroactive species.

The exploration of surface coverage during a deposition processes requires the use of volumetric sweeps that are capable of passively attenuating electroactive molecules on the surface without influencing the rate of deposition. In order to ascertain the relative surface coverage, Cyclic Voltammograms (CV) produce measurements of the surface molecule's oxidation and reduction. Then are integrated generating the measurement of Coulombic charge required to oxidize or to reduce the surface. Using CVs without effecting deposition necessitates low concentrations of adsorbing species in solution on the order of a few micromoles per liter.⁵⁻⁶ Of course CVs also are able to measure changes in the surface following the desorption of electroactive species.⁶ Thus monitoring the rate of deposition and desorption provide insight into the effects of surface interactions on these processes.

adsorptions relied on the repulsion of adsorbed species to that of those in solution. The electrostatic forces were dictated by the potential charge of the electrode and surface interactions due to adsorption. Thus the coverage of molecules on the surface of the electrodes were examined by sweeping the voltage and determining number of bound molecules through signal

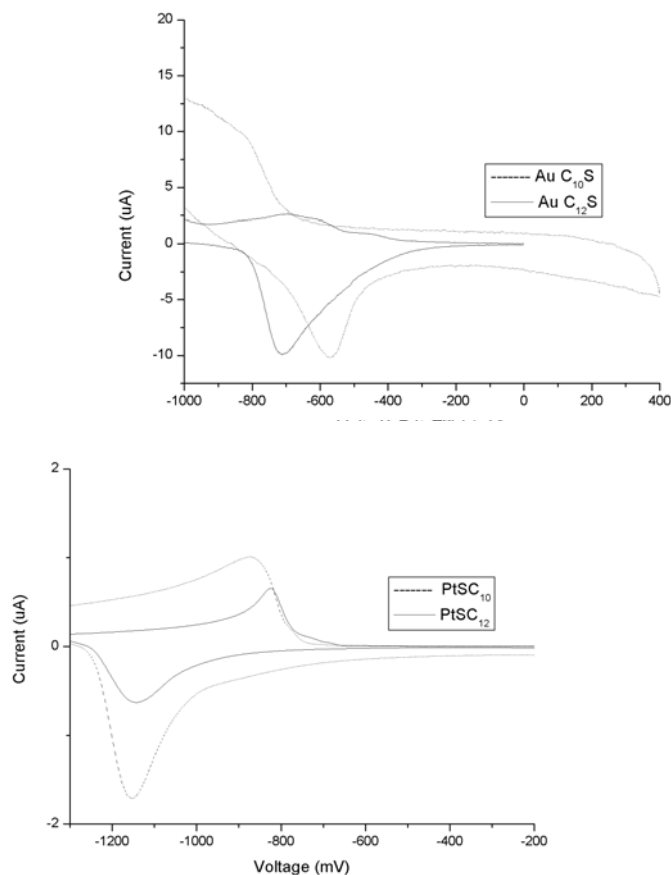


Figure 4.3. Cyclic Voltammograms of the reductive desorption of dodecane and decane thiol monolayers on gold and platinum substrates labeled respectively. Taken at a scan rate of 100mV s^{-1} , after 3 hours of under potential deposition at -200mV .

4.3. Electrochemical Desorption on Platinum and Gold Substrates

As shown previously with the reductive desorption of alkanethiolates on Au(111), experimentation into the feasibility of comparing various substrates and chain length were conducted to characterize surface interactions between respective metals and thiols. However unlike previously experiments the use of multifaceted beads similar to those used in STM experiment created an approximation of (111) plane surfaces.¹⁻³ With the adaptation of polycrystalline substrates, limitation with in the solvent window became

apparent as all 0.1mM KOH in ethanol yielded identical CVs that lack any desorption peaks. Therefore the use of dimethylfuran within a nitrogen atmosphere provided a shift in the solvent window and an absence of water.⁷ Upon sweeping a potential range of 400mV to -1800mV reductive desorption peak were seen for both platinum and gold substrate using dodecanethiol and decanethiol. Also a shift in potential with respect to chain length demonstrated similar characteristics to that of previously reported experimentation for gold substrates.¹⁻³ However, a potential shift of -40mV for the two methylene units differences were not observed. Instead a shift of -140mV for gold and -10mV for platinum monolayers were found. Suggesting that the use of polycrystalline surface failed to approximate (111) lattices used in literature. Yet the observation of platinum's -443mV shift with respect to that of gold suggested a consistency with that of RL data. The lack of similarities between that of platinum and gold desorption suggested further adjustment of experimental parameter was needed.

4.4. Conclusions

The use of electrochemistry to provide a means of verifying conclusions based on lithographic interpretations of surfaces response allows insight into potentially driven processes. While the use of the reductive desorption model in electrochemistry augments the observable behaviors produced by RL, the variations within monolayer preparation prevents a direct correlation between experiments. The use of electroactive species adsorbed on various substrates presents avenues into investigating adsorption and desorption rate dependent phenomenon. Thus using reductive desorption to interpret effects of monolayer structure on its stability produces a practical approach to studying substrate effects on molecular electronics. **However, through recent studies the**

applicability of current data presented in this chapter lacks the proper characterization needed to produce insight into replacement lithography and represents a speculative study of reductive desorption of thiols on various substrates.

4.5. Experimental Procedure

Substrates were obtained from Alfa Aesar and prepared from 0.5mm diameter Au(99.999%) and Pt(99.95%). Thiol solutions were created using n-dodecane thiol 98% and n-decane thiol (neat) diluted to 4.0mM in 10mM tetraethylammonium tetrafluoroborate ((C₂H₅)₄NBF₄) and dimethylfuran(DMF) obtained from Aldrich. Gold substrate preparation consisted of annealing on end of the wire with a H_{2(g)}/O_{2(g)}, followed by immersing in piranha solution for several minutes and rinsed off with distilled water. In order to create the highest facet coverage possible required annealing for 15 minutes with a H_{2(g)} flame; afterwards, the samples were placed under vacuum and transferred into a N_{2(g)} dry box. Platinum samples were prepared by annealing with a H_{2(g)}/O_{2(g)} for 15 minutes followed by immersing in concentrated hydrochloric acid for 15 minutes. After rinsing with distilled water and ethanol samples were dried under a N_{2(g)} stream; then placed under vacuum and transferred into a N_{2(g)} dry box.

Samples prepared under previously mentioned procedures were setup within an electrochemical cell that used Pt wire 99.95% purity 0.5mm diameter as counter and quasi-reference electrodes. Substrates were set as the working electrode so that the majority of the annealed ball remained under thiol solution. Initial conditions of electrochemical potentials were set at 200mV to -1600mV for gold and 400mV to

-1800mV for platinum. Once setup an initial scan was taken it was followed by three hours of under potential deposition at -200mV, and the reductive desorption scan was then taken. Afterwards, a photograph of the setup was taken to approximate the surface area of the electrode in solution. Reductive data was then scaled so that multiple chain lengths could be compared on the same graph.

4.6. References

- (1) T. Kakiuchi, H. Usui, D. Hobara, M. Yamamoto. *Langmuir* 18 (2002) 5231-5238.
- (2) C. Widrig, C. Chung, M. Porter, J. *Electroanal. Chem.* 310 (1991) 335-359.
- (3) T. Sumi, H. Wano, K. Uosaki. *J. Electroanal. Chem.* 550-551 (2003) 321-325.
- (4) R. Bretz, H. Abruña. *J. Electroanal. Chem.* 388 (1995) 123-132.
- (5) R. Bretz, H. Abruña. *J. Electroanal. Chem.* 408 (1996) 199-211.
- (6) R. Brito, R. Tremont, O. Feliciano, C. Cabrera J. *Electroanal. Chem.* 540 (2003) 53-59.
- (7) T. Schneider, D. Buttry. *J. Am. Chem. Soc.* 115 (1993) 12391-12397.

Appendix I

Schemes of STM Cell Design

AI.1 Standard Cell Design

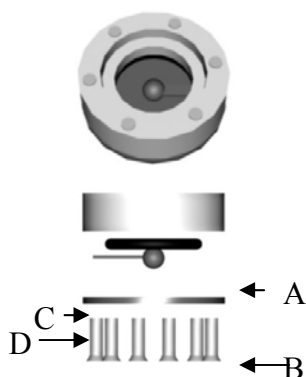


Figure A1.1. Schematic of basic STM Cell design using platinum ball with foil stem A) Teflon well with hollow center and recessed inner ring. B) Ferromagnetic stainless steel disc 6 holed for screw attachment to Teflon well. C) Rubber o-ring used to create leak resistant seal. D) Platinum ball with foil stem

The Standard STM Cell setup commonly used with platinum disked based setup where the metal of interest is attached to a platinum base by a metal common to the substrate. However, the foil of the platinum substrate prevents the creation of leak resistant seal.

AI.2 Raised Bolt Cell Design

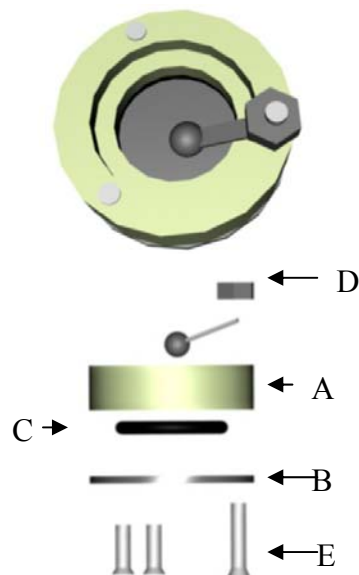


Figure A1.2. Schematic of raised bolt STM Cell design using platinum ball with foil stem A) Teflon well with hollow center and recessed inner ring. B) Ferromagnetic stainless steel disc 6 holed for screw attachment to Teflon well. C) Rubber o-ring used to create leak resistant seal. D) Stainless steel nut used to secure platinum foil to setup E) Elongated metallic screw.

The Raised Bolt design prevented the leakage of the standard cell design; yet the distance from the anchoring point to the substrate generated of noise within the image.

AI.3 Imbedded Cell Design

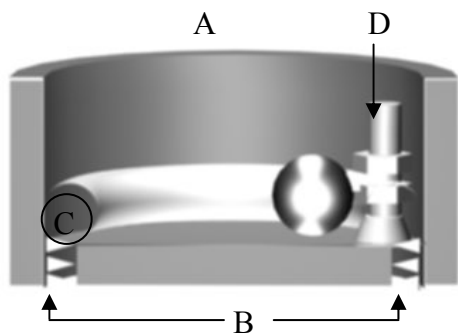


Figure AI.3. Imbedded Screw design. A) Casing of an AFM cell with threaded bottom inner shaft. B) Threaded bottom for mounting screw. C) Epoxy Seal to secure screw and prevent leakage. D) Screw and nut imbedded in epoxy to anchor the substrate.

In order to limit the leakage of dodecane and allow the attachment of the platinum substrate as close to the anchor point as possible an Imbedded Cell design was chosen. The Ferromagnetic disk was used to stabilize the cell and reduce the amount of noise generated from the scanning process. The use of epoxy was meant to prevent leakage; but solvent resistant epoxy was not chosen and no replacement was observed. The epoxy also dissolved in ethanol and dodecane make a

reconstruction of the cells after several

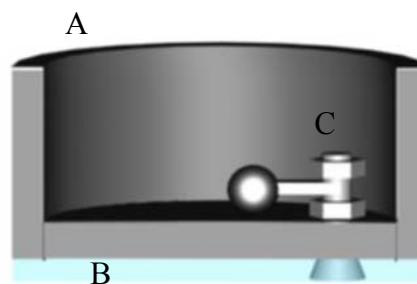


Figure AI.4. Sealed Cell Design. A) Machined metal casing made from ferromagnetic stainless steel. The bottom of which contains a hole for the screw. B) Resin solder used to seal the bottom of the cell and secure the screw. C) Standard Screw bolt design with platinum foil.

uses.

AI.4 Sealed Cell Design

The Sealed Cell Design provides a sealable environment to prevent leakage of dodecane and provides a securable anchor in close proximity to the substrate. The resin solder creates a seal on the bottom of the cell; yet, the application of the solder reduces the contribution of the magnet on the peizo to stabilize the sample. Also the application of the solder and head of the screw on the bottom angled the sample and made alignment more difficult.

AI.5 Never Leak Cell Design

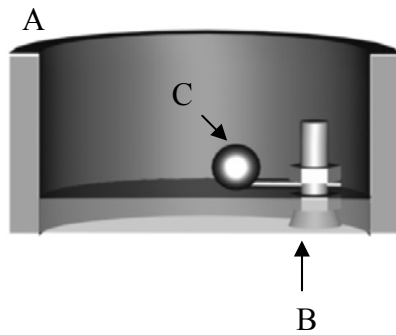


Figure AI.5. Never Leak Design. A) Machined metal casing made from ferromagnetic stainless steel. The bottom of which contains a threaded hole for the screw with a beveled bottom. B) Screw sealed with conductive ink. C) Platinum or Palladium Substrate using a wire based form of attachment.

The Never Leak Cell design

provided corrections to all problems previously mentioned with other designs. Also the use of annealed wire reduced the amount of vibrational noise generated by the malleability of foil stems. The use of conductive ink provided a means of sealing the cell without causing any alignment issues.

Appendix II

Schemes of

Electrochemical Electrode

AII.1. Indium Contact Electrode

Figure AII.1. Indium Contact Electrode. A) Copper wire used to make electrical contact. B) Substrate of choice: Pt, Pd, or Au. C) Indium melted to form back contact



AII.2. Silver Contact Electrode



Figure AII.2. Silver Conductive Ink Electrode. A) Copper wire used to make electrical contact. B) Tygon tubing used to secure electrode to cell setup. C) Glass casing used to deliver conductive ink and shield wiring. D) Conductive ink creating interface between substrate and copper wiring. E) Substrate.

AII.3. Top Contact Electrode

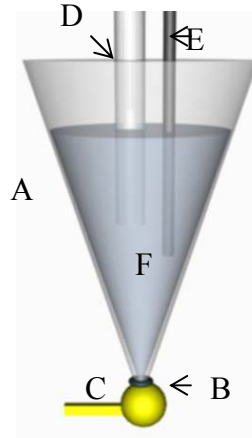


Figure AII.3. Top Contact Electrode. A) Glass cell created by melting the end and sanding end to reveal micron size hole. B) Vacuum Grease sealant. C) Annealed so that faceted surface aligns with glass frit D) Reference electrode. E) Counter electrode. F) Electrolyte solution.

AII.4. Plasti™-Dip Electrode

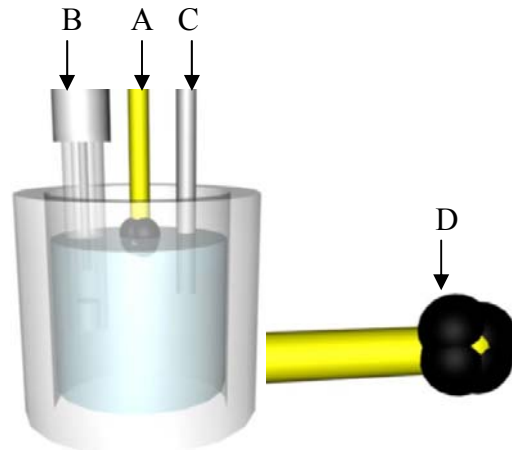


Figure AII.4. Plasti™-Dip Electrode A) Working Electrode. B) Reference electrode. C) Counter electrode. D) Plasti™-Dip coating isolates electrolyte solution and limits exposure to faceted region.

AII.5. DMF Annealed Electrode

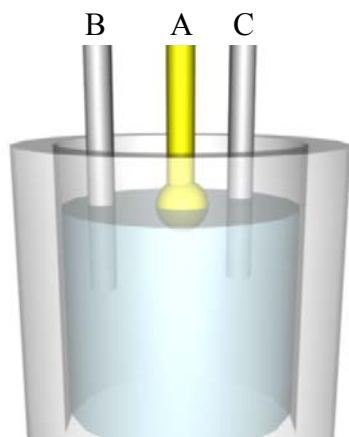


Figure AII.5. A) Flame annealed ball for 15 min to maximize faceted regions. B) Counter electrode. C) Quasi-reference electrode (Pt wire).

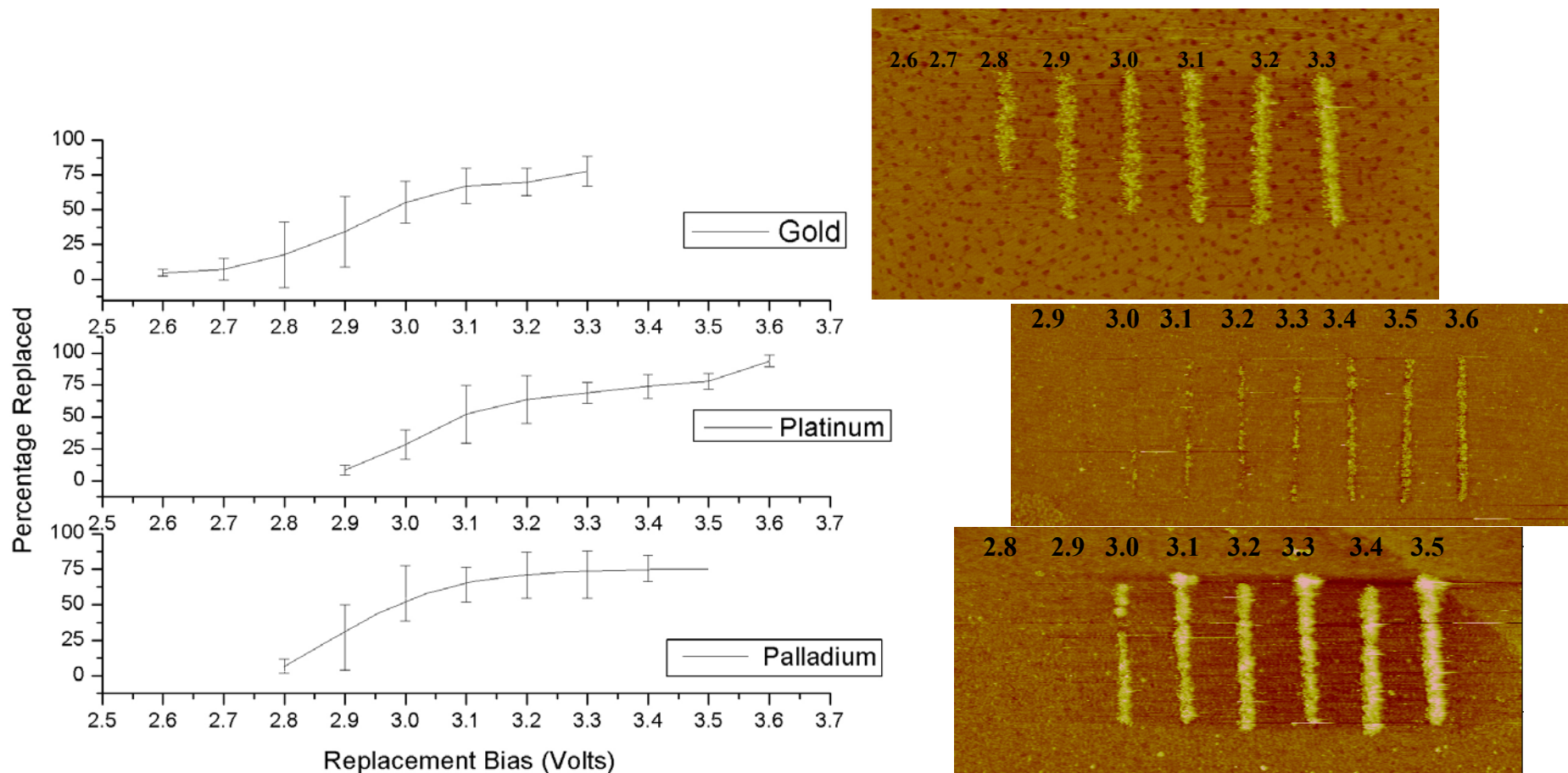


Figure 3.4 A graphic representation of the Percentage of Fc-C₁₁SAC Replacement versus Replacement Bias (the line is meant to guide the eye through mean percentage of each bias). Adjacent images represent data points for the graph with lines generated as a result of Voltage biases listed above each line with respective substrate indicated by adjacent labeled graph. Gold, platinum, and palladium substrate imaging conditions $V_{\text{bias}}=1.7\text{V}$ scale= 350nm^2 , $V_{\text{bias}}=1.9\text{V}$ scale= 400nm^2 , $V_{\text{bias}}=1.7\text{V}$ scale= 350nm^2 respectively. All setpoint and Z-scale were 10pA and 3nm.

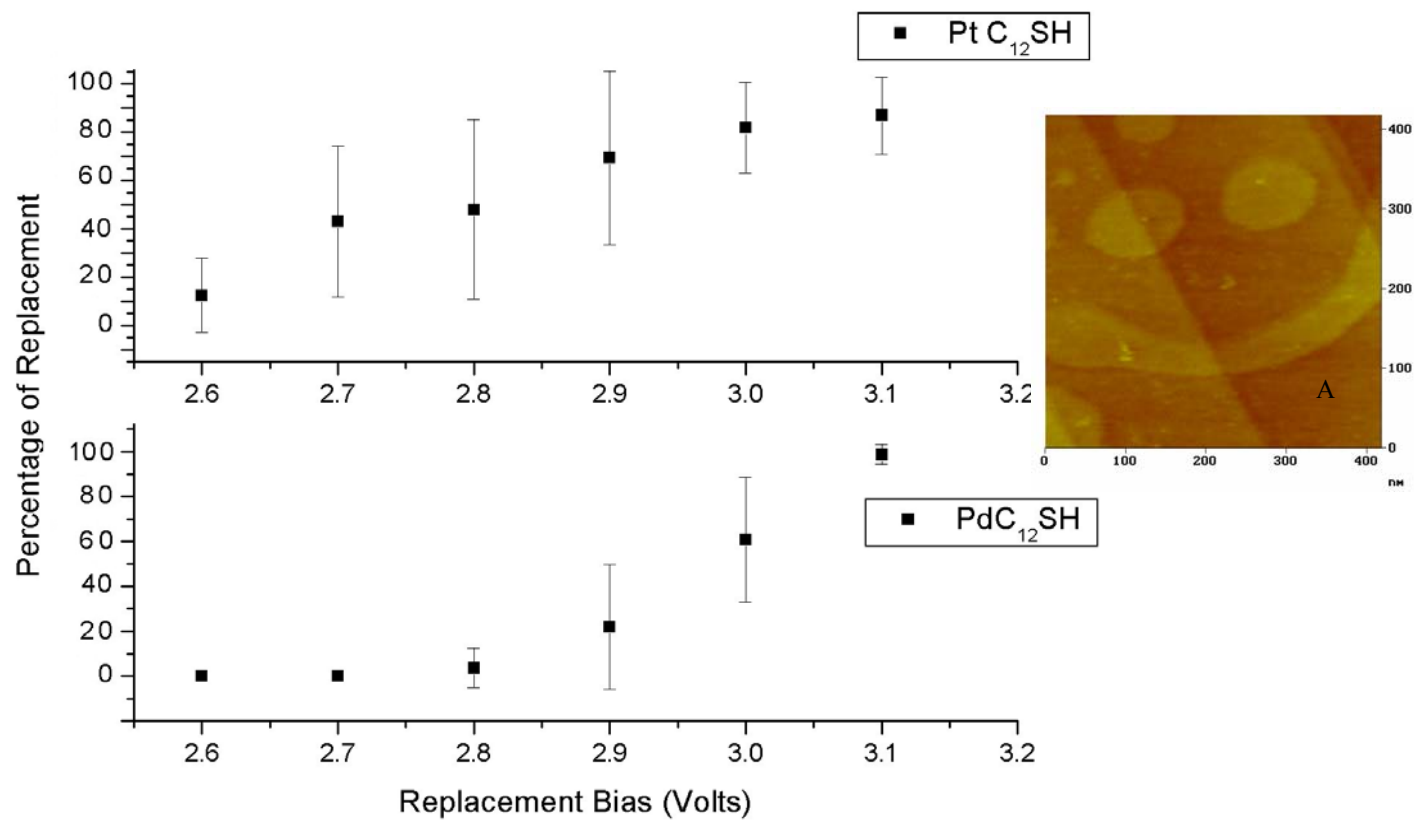


Figure 3.5 Graphs of Percentage of Fc-C₁₁SAC Replacement versus Replacement Bias of un-etched platinum and palladium. A) Pd C₁₂S monolayer imaged at 1.0V, setpoint 10pA, scan size 400 nm², and 3nm Z-scale.